Forest Ecology and Management 555 (2024) 121729

Contents lists available at ScienceDirect

Forest Ecology and Management

journal homepage: www.elsevier.com/locate/foreco

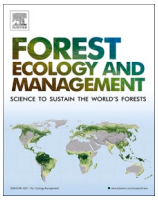

Integrating geospatial, remote sensing, and machine learning for climate-induced forest fire susceptibility mapping in Similipal Tiger Reserve, India

Chiranjit Singha [a], Kishore Chandra Swain [a], Armin Moghimi [b], Fatemeh Foroughnia [c,*], Sanjay Kumar Swain [a]

[a] Department of Agricultural Engineering, Institute of Agriculture, Visva-Bharati (A Central University), Sriniketan, Birbhum, West Bengal 731236, India
[b] Ludwig-Franzius Institute of Hydraulic, Estuarine and Coastal Engineering, Leibniz University Hannover, Nienburger Str. 4, 30167 Hannover, Germany
[c] Department of Geoscience and Engineering, Civil Engineering and Geosciences Faculty, Delft University of Technology, Delft, The Netherlands

ARTICLE INFO

Keywords:
Forest fire
Machine learning
Susceptibility map
Boruta-SHAP
Risk map

ABSTRACT

Accurately assessing forest fire susceptibility (FFS) in the Similipal Tiger Reserve (STR) is essential for biodiversity conservation, climate change mitigation, and community safety. Most existing studies have primarily focused on climatic and topographical factors, while this research expands the scope by employing a synergistic approach that integrates geographical information systems (GIS), remote sensing (RS), and machine learning (ML) methodologies for identifying and assessing forest fire-prone areas in the STR and their vulnerability to climate change. To achieve this, the study employed a comprehensive dataset of forty-four influencing factors, including topographic, climate-hydrologic, forest health, vegetation indices, radar features, and anthropogenic interference, into ten ML models: neural net (nnet), AdaBag, Extreme Gradient Boosting (XGBTree), Gradient Boosting Machine (GBM), Random Forest (RF), and its hybrid variants with differential evolution algorithm (RF-DEA), Gravitational Based Search (RF-GBS), Grey Wolf Optimization (RF-GWO), Particle Swarm Optimization (RF-PSO), and genetic algorithm (RF-GA). The study revealed high FFS in both the northern and southern portions of the study area, with the nnet and RF-PSO models demonstrating susceptibility percentages of 12.44% and 12.89%, respectively. Conversely, very low FFS zones consistently displayed susceptibility scores of approximately 23.41% and 18.57% for the nnet and RF-PSO models. The robust mapping methodology was validated by impressive AUROC (>0.88) and kappa coefficient (>0.62) scores across all ML validation metrics. Future climate models (ssp245 and ssp585, 2022–2100) indicated high FFS zones along the northern and southern edges of the STR, with the central zone categorized from low to very low susceptibility. Boruta analysis identified actual evapotranspiration (AET) and relative humidity as key factors influencing forest fire ignition. SHAP evaluation reinforced the influence of these factors on FFS, while also highlighting the significant role of distance to road, distance to settlement, dNBR, slope, and humidity in prediction accuracy. These results emphasize the critical importance of the proposed approach for forest fire mapping and provide invaluable insights for firefighting teams, forest management, planning, and qualification strategies to address future fire sustainability.

1. Introduction

The escalating frequency of forest fires worldwide is a concerning natural and anthropogenic phenomenon (Zema et al., 2020). In 2021, global wildfires led to the loss of approximately 7.02 million hectares of tree cover (Dos Reis et al., 2021). According to the Forest Survey of India, from November 2021 to June 2022, India experienced 223,333 forest fires, resulting in a substantial loss of 3.59 lakh hectares of forest cover [Source: Jayashree Nandi, India News (URL: https://www.hindustantimes.com/india-news/increasing-intensity-global-forest-fires-burning-twice-as-much-tree-cover-climate-crisis-to-blame-101693563239463.html). Forest fires in India typically occur from mid-February to the end of June. These events profoundly impact the atmosphere, soil ecology, biodiversity, and human health in forested areas

* Corresponding author.
E-mail address: f.foroughnia@tudelft.nl (F. Foroughnia).

https://doi.org/10.1016/j.foreco.2024.121729
Received 18 October 2023; Received in revised form 21 January 2024; Accepted 22 January 2024
Available online 31 January 2024

(Mutthulakshmi et al., 2020). Furthermore, climate change, including declining precipitation, rising temperatures, and increased drought frequency, has significantly contributed to the surge in forest fire incidents (Keenan, 2015). Concurrently, human activities contribute to the occurrence of wildfires reciprocally (Simioni et al., 2020). Therefore, developing fire susceptibility maps in the early stages is crucial for identifying potential risks and anticipating their consequences on social infrastructure and the environment (Ghorbanzadeh et al., 2019). These maps are also invaluable resources for reducing forest vulnerability and enhancing the decision-making process for ecological risk mitigation (Gong et al., 2022). Many of these risk maps can be generated by using several conditioning factors of forest fires, mainly derived from geographical information systems (GIS) and remote sensing (RS) systems, or their integration (Lamat et al., 2021). Numerous studies have explored the impact of these factors on mapping forest fire susceptibility (FFS). These studies consider a range of elements, including climatic factors such as temperature, rainfall, humidity, and wind speed, alongside geo-environmental factors like altitude, aspect, slope, river presence, Topographic Wetness Index (TWI), and land use patterns (Lamat et al., 2021; Arca et al., 2020; Tiwari et al., 2021; Moayedi et al., 2020).

The rapid advancement of computational capabilities has fueled the development of enhanced machine learning (ML) models, enabling their integration with RS and GIS to produce more accurate and reliable FFS maps (Tang et al., 2020; Mabdeh et al., 2022; Rihan et al., 2023). ML techniques offer a distinct advantage over traditional statistical methods in handling high-dimensional and complex nonlinear datasets, leading to their growing adoption in FFS mapping research rather than statically models (Kantarcioglu et al., 2023; Sivrikaya and Küçük, 2022; Pham et al., 2020). Over the past decade, a growing body of research has utilized single- or multi-modal ML techniques to evaluate and optimize FFS mapping methodologies, consistently demonstrating their effectiveness in enhancing map precision (Shi and Zhang, 2023; Piao et al., 2022; Mohajane et al., 2021; Trucchia et al., 2022; Saha et al., 2023). In such research works, the algorithms used for FFS mapping analysis, including Artificial neural networks (ANN) (Gholamnia et al., 2020), Support vector machines (SVM) (Singh et al., 2021), Random Forest (RF) (Eskandari et al., 2020), Generalized Additive Model (GAM) (Pourtaghi et al., 2016), Classification and Regression Tree (CART) (Sulova and Joker Arsanjani, 2021), Gradient Boosting Machine (GBM) (Achu et al., 2021), Dynamic Bayesian Network (DBN) (Pourghasemi et al., 2020), Logistic Regression (LR) (Shabani et al., 2020), Xtreme Gradient Boosting (XGB) (Akıncı et al., 2023), Naïve Bayes Tree (NBT) (Jaafari et al., 2018), Multivariate Adaptive Regression Splines (MARS) (Tien et al., 2019), LogitBoost Ensemble-based Decision Tree (LEDT) (Tehrany et al., 2019).

Recently, there has been a notable surge in interest regarding the application of cloud-based platforms such as Google Earth Engine (GEE), particularly in hazard prediction and wildfire susceptibility assessment (Jaafari et al., 2018; Amani et al., 2020; Tavakkoli et al., 2022). For example, Sharma et al. (2022) employed ANN and RF for the FFS classification within GEE with topography and climate factors for forest fire hotspot identification in India between 2001 and 2020. The results highlighted the superior performance of the ANN model, achieving an impressive Area Under the Curve (AUC) of 90%, surpassing other models considered. In another effort, Babu et al. (2023) introduced a GEE-based FFS map for Indian forests. Considering 14 factors from RS and GIS, including topography, vegetation, climate, and anthropogenic interferences, they employed six ML algorithms (ANN, RF, maximum entropy, generalized linear model, MARS, GBM) and their ensemble models. The results indicated accurate predictions of fire occurrence for all six ML algorithms, achieving a high accuracy with an AUC $>$ 90%. Moreover, around 27% of the total area was identified as having a high to very high fire risk due to landscape factors.Abdollahi and Pradhan (2023) used 29 environmental parameters along with Explainable Artificial Intelligence (XAI)-enabled Deep Neural Network (DNN) and Maximum Entropy (MaxEnt) models for wildfire susceptibility mapping in Nepal, achieving a very high AUC value of 94% in detecting forest fire incidents from 2017 to 2019. In another study done by Mohajane et al. (2021) in a Mediterranean region, five ML models based on Multi-Criteria Decision Making (MCDM) and Frequency Ratio (FR) were used with 510 fire inventory events and 10 independent causal factors. Their evaluation revealed that RF achieved the highest accuracy with an AUC of 98%, followed by SVM-FR (AUC = 95%), MLP-FR (AUC = 85%), CART-FR (AUC = 84%), and LR-FR (AUC = 80%). Iban and Sekertekin (2022) also employed multiple ML models, such as SVM, LR, LDA, GBM, XGB, RF, and AdaBoost (AB), to map FFS distribution in the Mediterranean Region of Turkey. The study focused on four main factors: climatological, topographical, vegetation, and anthropogenic. Notably, the RF model demonstrated superior performance, achieving an AUC of 0.801, with 7.20% of the area classified as having a very high FFS. Considering eight factors, Sun et al. (2022) utilized RF, LR, and LightGBM ML methods for FFS mapping in China's Jiangsu province. The results indicated that the LightGBM model (AUC of 88.8%) outperformed the RF and LR models.

While single ML models have shown promise in previous studies, hybrid ML approaches have emerged as a compelling alternative for achieving enhanced FFS mapping accuracy in specific regions (Jain et al., 2020). These hybrid approaches combine the strengths of multiple ML algorithms, which can effectively address the intricate nonlinearities inherent in geographical challenges. For instance, Mabdeh et al. (2022) employed hybrid ML models in Ajloun, Jordan, incorporating 100 wildfire points and 13 fundamental factors. Their findings revealed that the SVR-based Genetic Algorithm (GA) model achieved the highest AUC for FFS mapping. In another study, Moayedi and Khasmakhi (2023) evaluated the performance of ANNs coupled with Biogeography-Based Optimization (BBO) and evolutionary Ant Colony Optimization (ACO) to predict FFS zones in Golestan Province, Iran. The results demonstrated that ACO-ANN and BBO-ANN methods (AUCs of 0.879 and 0.937, respectively) yielded superior results in forecasting FFS using 15 forest fire conditioning factors. Studies by Mohajane et al. (2021), Shi and Zhang (2023), Jain et al. (2020), and Singha et al. (2022) have also highlighted the effectiveness of hybrid ML models in improving FFS mapping accuracy.

Despite the ongoing developments in hybrid ML models, a noticeable gap persists in the existing literature. While some research has been conducted on assessing and predicting FFS in specific regions using these techniques, there is a distinct lack of inclination toward investigating the performance of ML models in mapping FFS under future climate-induced scenarios. On the other hand, researchers have frequently turned to general circulation models (GCMs) to assess the impacts of climate change on fire danger (Barnard et al., 2023). For example, Gallo et al. (2023) examined global fire weather indicators using 16 GCMs from the Coupled Model Intercomparison Project (CMIP6), demonstrating that carefully selecting and evaluating GCMs can significantly improve the accuracy of projections related to climate-induced wildfire risk. However, despite their potential, GCMs have faced criticism for inherent limitations, including resolution constraints, complexity, and computational intensity in assessing climate change impacts on fire danger.

In another aspect, the Similipal Tiger Reserve (STR), known as a rich biodiverse natural haven in eastern India (Dash and Behera, 2018), witnessed a devastating wildfire in 2021 that raged for over two weeks [Source: URL: https://www.thehindu.com/news/national/other-states/simlipal-park-fire-under-control-rainfall-helps/article34051180.ece]. This incident resulted in widespread environmental damage and the displacement of wildlife into neighboring human habitations [Source: Mohammad Suffian, India Today. URL: https://www.indiatoday.in/india/story/habitat-burnt-in-simlipal-forest-fire-wild-animals-enter-human-areas-in-odisha-1777385–2021-03–09]. Despite this alarming event, there is no extensive research on ML-based mapping for STR and its potential implications under future climate change in this region. Therefore, a comprehensive examination of hybrid/single ML models'

ability to clarify current and future forest fire patterns through FFS mapping under projected future climate conditions in STR is essential, which the present study intends to do.

Accordingly, the main contributions of the study are listed as follows:

1) A novel ML-nature-inspired ensemble framework is presented for Forest Fire Susceptibility (FFS) assessment and forecasting in the STR. This methodology employs several advanced ML models (i.e., neural net (nnet), AdaBag, Extreme Gradient Boosting (XGBTree), GBM, RF, RF fine-tuned by differential evolution algorithm (RF-DEA), Gravitational Based Search (RF-GBS), Grey Wolf Optimization (RF-GWO), Particle Swarm Optimization (RF-PSO), and genetic algorithm (RF-GA)), to predict FFS zones using 44 independent Remote Sensing (RS) and Geographic Information System (GIS)-derived factors. These factors are spatially grouped into topographic, climate-hydrologic, radar features, vegetation indices, and anthropogenic interference parameters. This contribution is expected to provide a more accurate and detailed understanding of forest fire risks in the STR.
2) The resulting FFS map is integrated with future climatic scenarios from the CMIP6 dataset, utilizing socio-economic pathways (ssp245 and ssp585) to create future FFS trends. This integration allows for a more comprehensive assessment of current and future forest fire trends from 2022 to 2100. By incorporating future climate projections, the study provides a forward-looking and insightful assessment of forest fire risks, aiding in long-term planning and mitigation strategies.

2. Materials and methods

2.1. Study area

The STR in Odisha, India, covers an area of ~ 2750 km^2 and was declared a UNESCO Biosphere Reserve in 2009 for its rich biodiversity. Its coordinates range from 86° 04' to 86° 38' E longitude and 21° 29' to 22° 16' N latitude (Fig. 1(a)). The average altitude of the region is 900 m and it is mainly covered by teak (Sal) forests. Annual rainfall varies from 1200 mm to 2000 mm, and temperatures range from 9 °C to 33.5 °C. Recent years have witnessed extensive forest conversion to agriculture, mining, and human settlements, intensifying deforestation, fires, and hunting. Notably, most fires occur in March and April, with peak burn areas in 2012 and 2014 (Fig. 1(b)). [Source: URL:https://gwis.jrc.ec.europa.eu/applications].

2.2. Forest fire inventory

This study used the GEE-based FIRMS (Fire Information for Resource Management System) in conjunction with the LANCE (Land, Atmosphere Near real-time Capability for EOS) fire detection system to collect forest fire inventory data spanning from 2012 to 2022 (URL: https://www.earthdata.nasa.gov/). A total of 500 forest fire locations

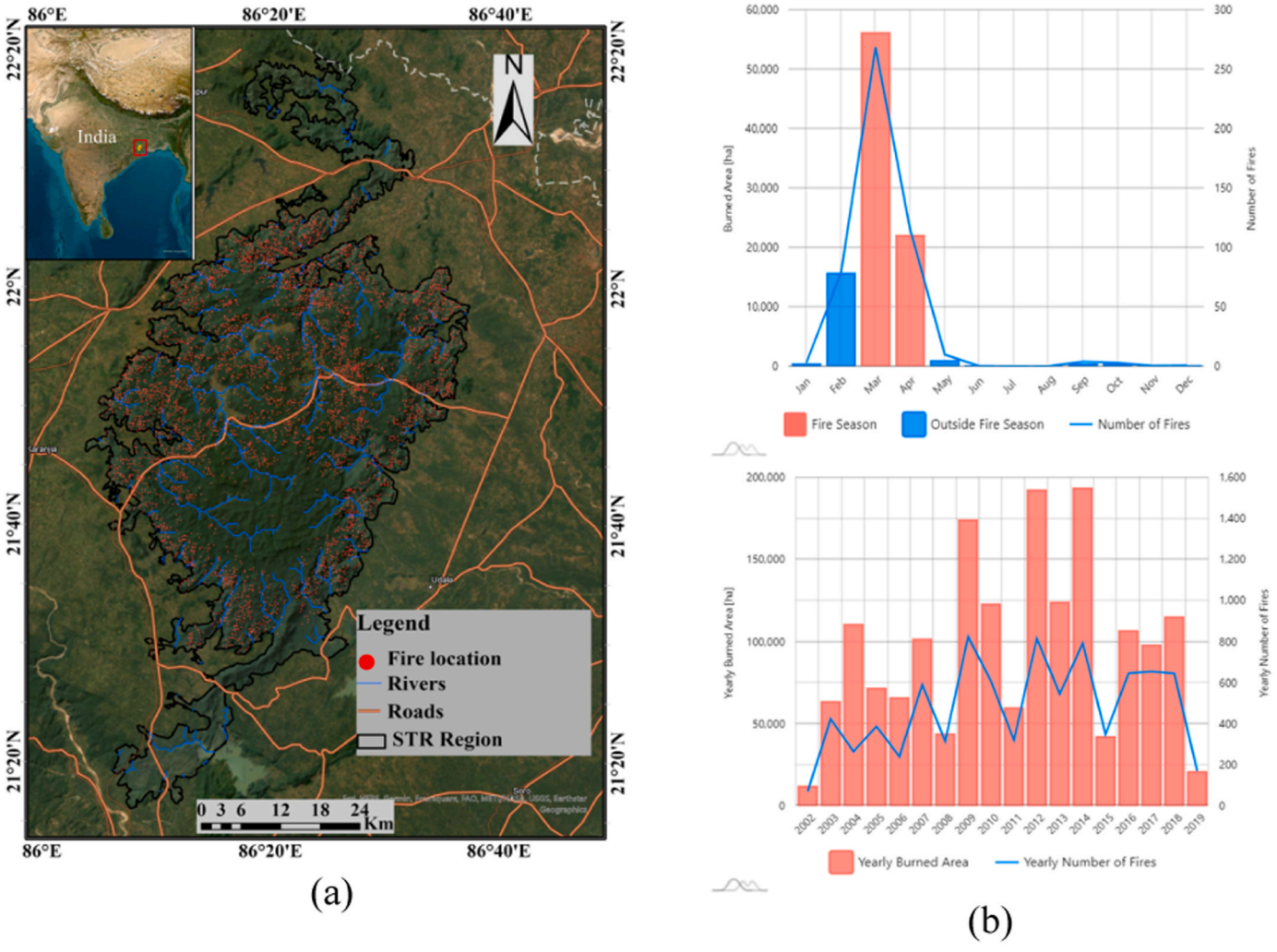

Figure1. (a) Study area distribution map, and (b) its fire seasons.

were considered, obtained through GPS field surveys, sourced from both the Forest Survey of India (FSI) and the FIRMS database. Additionally, 500 random points were generated outside the fire zones using the ArcGIS environment. In the fire susceptibility model, inventory values were categorized as either zero (no fire incidence) or one (presence of fire incidence). The sample sizes for training and validation were divided into two groups with a 70% to 30% ratio.

2.3. Forest fire factors

The intensity and size of forest fires can be influenced by factors such as, climate, topography, fuel types, and human-made features, collectively known as contributing variables. These elements significantly affect the environmental damage caused by forest fires (Eskandari and Khoshnevis, 2020). This study assesses the correlation between various geo-environmental factors: topographic (Fig. 3), climate-hydrologic (Fig. 4), forest health (Fig. 5), vegetation indices (Fig. 6), radar features (Fig. 7), and anthropogenic interference (Fig. 8) in predicting FFS in the study area. Details of the selected fire conditioning factors have been provided in Supplementary material and Supplementary Table 1. All factors were resampled to a 10 m × 10 m resolution using the bilinear interpolation method in *R* software (Azmoon et al., 2022).

2.4. Methodology

The methodology follows a five-stage workflow (Fig. 2). First, using the GEE platform, a raster layer was created to map fire-ignition locations and to validate both fire and non-fire locations. Second, interrelationships among fire conditioning factors were assessed through Pearson correlation, Ordinary Least Squares (OLS), and multicollinearity tests. Moving on to the third stage, various Machine Learning (ML) algorithms (nnet, AdaBag, XGBTree, GBM, RF, RF-DEA, RF-GBS, RF-GWO, RF-GA, and RF-PSO) were implemented to predict final Fire Management Systems (FFS) maps in a spatial context. Following the ML implementation, the fourth stage involved the use of multiple statistical metrics, including accuracy, kappa coefficient, sensitivity, specificity, positive predictive values (PPV), and negative predictive values (NPV), to comprehensively evaluate the ML outcomes. Finally, in the fifth stage, the optimal model was utilized to project FFS into the future, considering two distinct CMIP6 (EC-Earth3) climate change scenarios (ssp245 and ssp585, 2022–2100).

2.4.1. Ordinary least square and Multicollinearity test

The selected fire ignition factors were analyzed linearly through coefficient estimation using the OLS method (Lee et al., 2022). The Variance Inflation Factor (VIF) was utilized to assess the extent of multicollinearity among the relevant variables (Singha et al., 2023). Besides, Pearson correlation was utilized to evaluate the spatial interconnectedness of the predictors' relationships.

2.4.2. Machine learning model application

As mentioned before, ten different ML algorithms were used in the present investigation. The optimal parameter settings for each of these models with a significant number of iterations and the best objective function value were determined before running the program (Supplementary Table 2, Supplementary Fig. 1). The considered ML models were described in the next subsections.

2.4.2.1. Random Forest (RF). RF algorithm, rooted in decision tree methodology, is a powerful tool for acquiring knowledge and making accurate forecasts based on data (Bustillo Sánchez et al., 2021). It excels in constructing models that capture complex correlations between input and output variables. In our specific case, the independent variables are referred to as predisposing factors, while the dependent ones are represented by the burned regions. RF functions with constructing a collection of decision trees, each trained on a distinct subset of the data, providing predictions that are then combined through averaging or voting to produce a final, accurate prediction (Breiman, 2001). The only

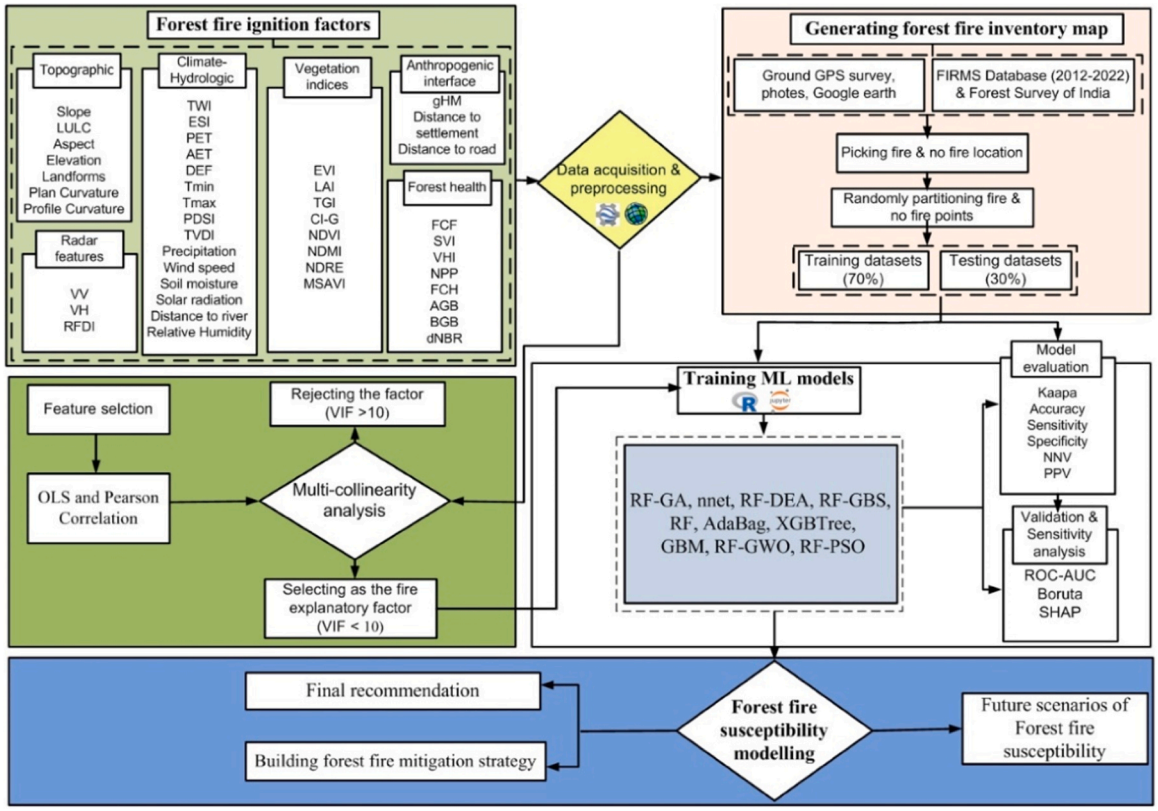

Fig. 2. Details workflow methodology for the FFS modelling.

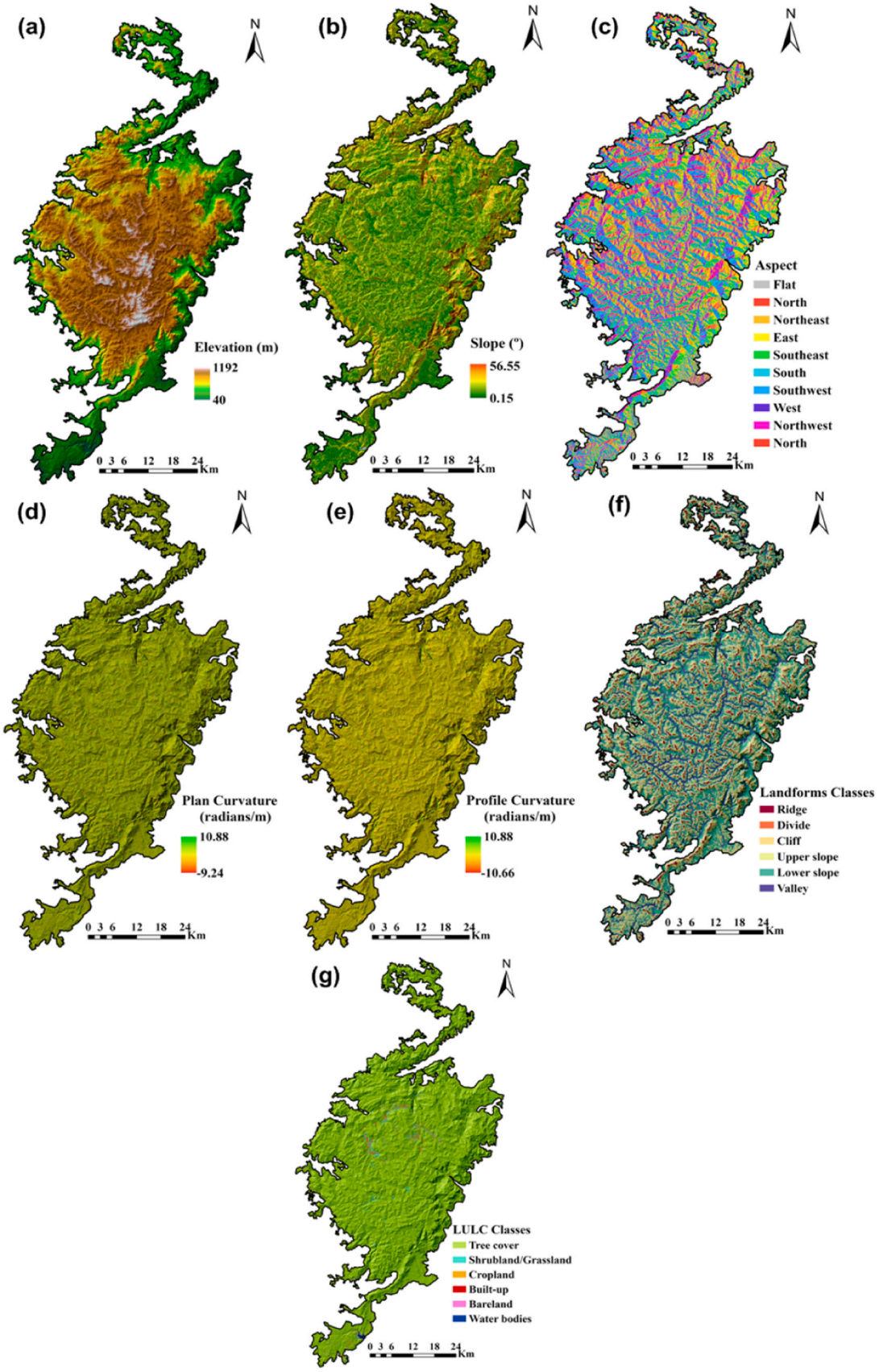

Fig. 3. Topographic factor maps, (a) elevation, (b) slope, (c) aspect, (d) plan curvature, (e) profile curvature, (f) landforms, and (g) LULC.

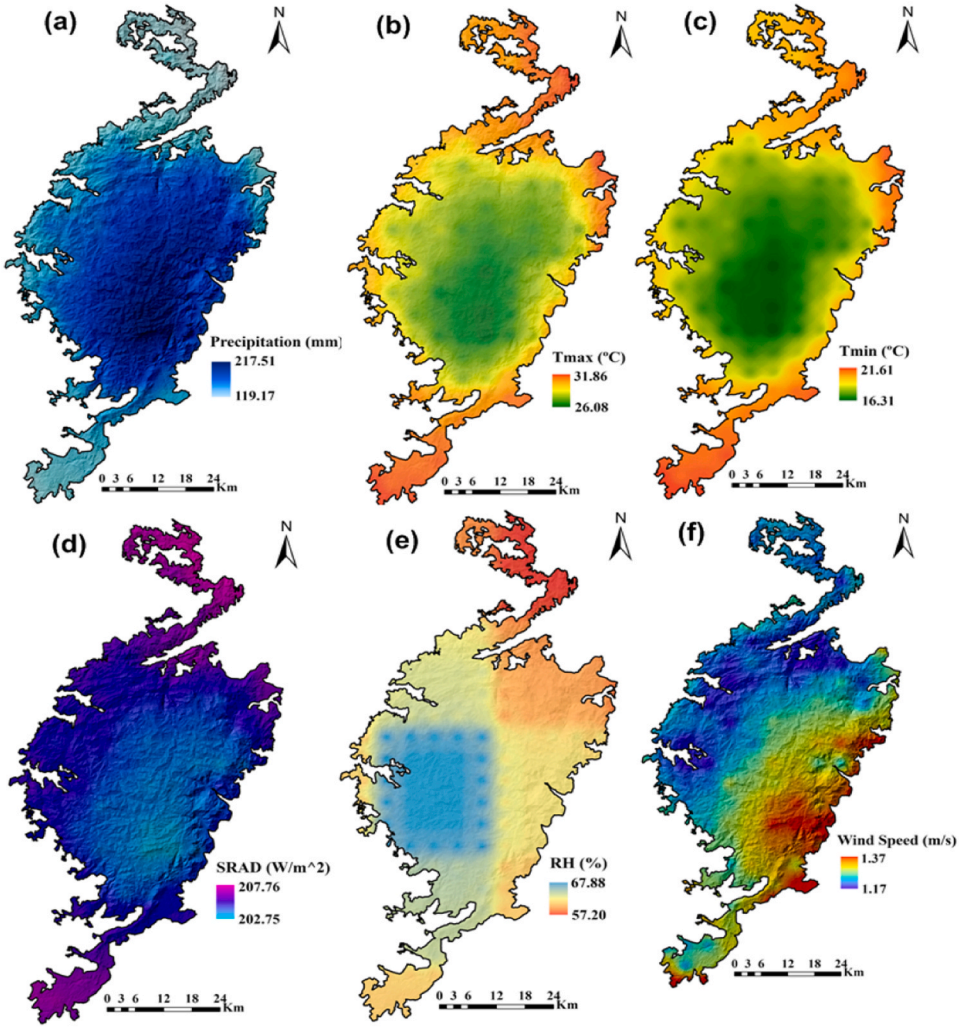

Fig. 4. Climate-hydrologic factors distribution map, (a) precipitation (b) tmax, (c) tmin, (d) SRAD, (e) RH, (f) wind speed, (g) AET, (h) PET, (i) DEF, (j) soil moisture, (k) ESI, (l) PDSI, (m) TVDI, (n) TWI, and (o) distance to river.

hyperparameters that require specification are user-defined, namely, the number of trees (*ntree*) needed for system implementation and the number of candidates for each split (*mtry*). In the current study, hyperparameters were fine-tuned to 500 for *ntree* and 5 for *mtry* (Supplementary Fig. 1).

2.4.2.2. Random Forest - Genetic Algorithm (RF-GA). RF parameters undergo a comprehensive evolution process within the GA, concerning crucial aspects like mutation rate, crossover rate, and selection (Elyan et al., 2017). The chromosome that perseveres through GA's evolutionary steps is identified as the most optimal parameter for the random forest (Li et al., 2016). Typically encoded as a binary string, each chromosome's effectiveness is assessed using a fitness function. Prior to modeling, GA fine-tunes the performance of RF IN FFS mapping. In this study, a thorough examination reveals the best RF parameter (i.e., *ntree*=512), which emerged after 19 iterations with a population size of 20 and a mutation rate of 0.1 (Supplementary Fig. 1).

2.4.2.3. Neural net (nnet). The nnet model is structured using the widely employed Perceptron architecture and the BackPropagation algorithm (Ghorbanzadeh et al., 2019). In this multi-layer framework, neurons within the same hidden layer do not possess connections. For a specific application, the size and number of hidden layers in the nnet model are typically predetermined. Initially, random weights are selected and then adjusted to minimize error. In this study, a network with layers configured as 43–20-2, comprising a total of 52 weights, was set for the nnet model.

2.4.2.4. Random Forest-Differential Evolution Algorithm (RF-DEA). DEA incorporates genetic operators for optimizations such as selection, crossover, and mutation (Das and Suganthan, 2011). This approach initiates by randomly generating a population with new candidate solutions acting as mutation operators. Subsequently, it executes crossover, selection, and crossover operations. If a termination criterion is met, the loop exits and the process reverts to creating new mutation vectors. In this study, we optimized the RF model utilizing the DEA. Through DEA evaluation, the best *ntree* was determined to be 489 (Supplementary Fig. 1).

2.4.2.5. Gravitational Based Search (RF-GBS). The GBS utilizes Newton's gravitational behavior (Rashedi et al., 2009). This framework allows users to define the objective function of the algorithm and return the value of the given model (Papa et al., 2011). It is useful in continuous optimization. The candidate solutions in a population are considered to have mass. They can then be updated through the second law of motion and the Newton law of gravity. This paper presents a method that combines the performance of the Optimum-Path Forest (OPF) classifier with the optimization achieved by the GSA. The goal is to provide a

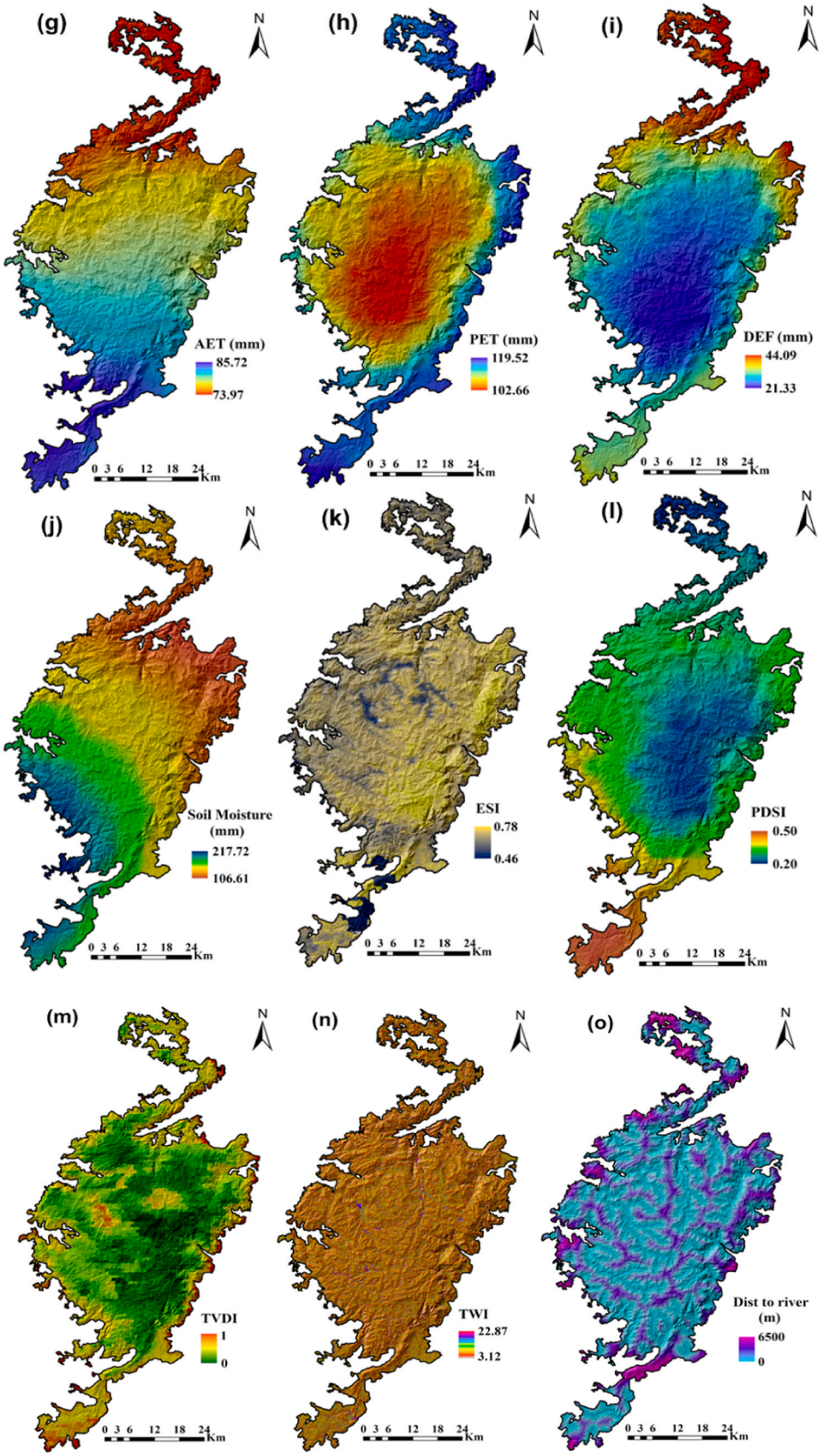

Fig. 4. (*continued*).

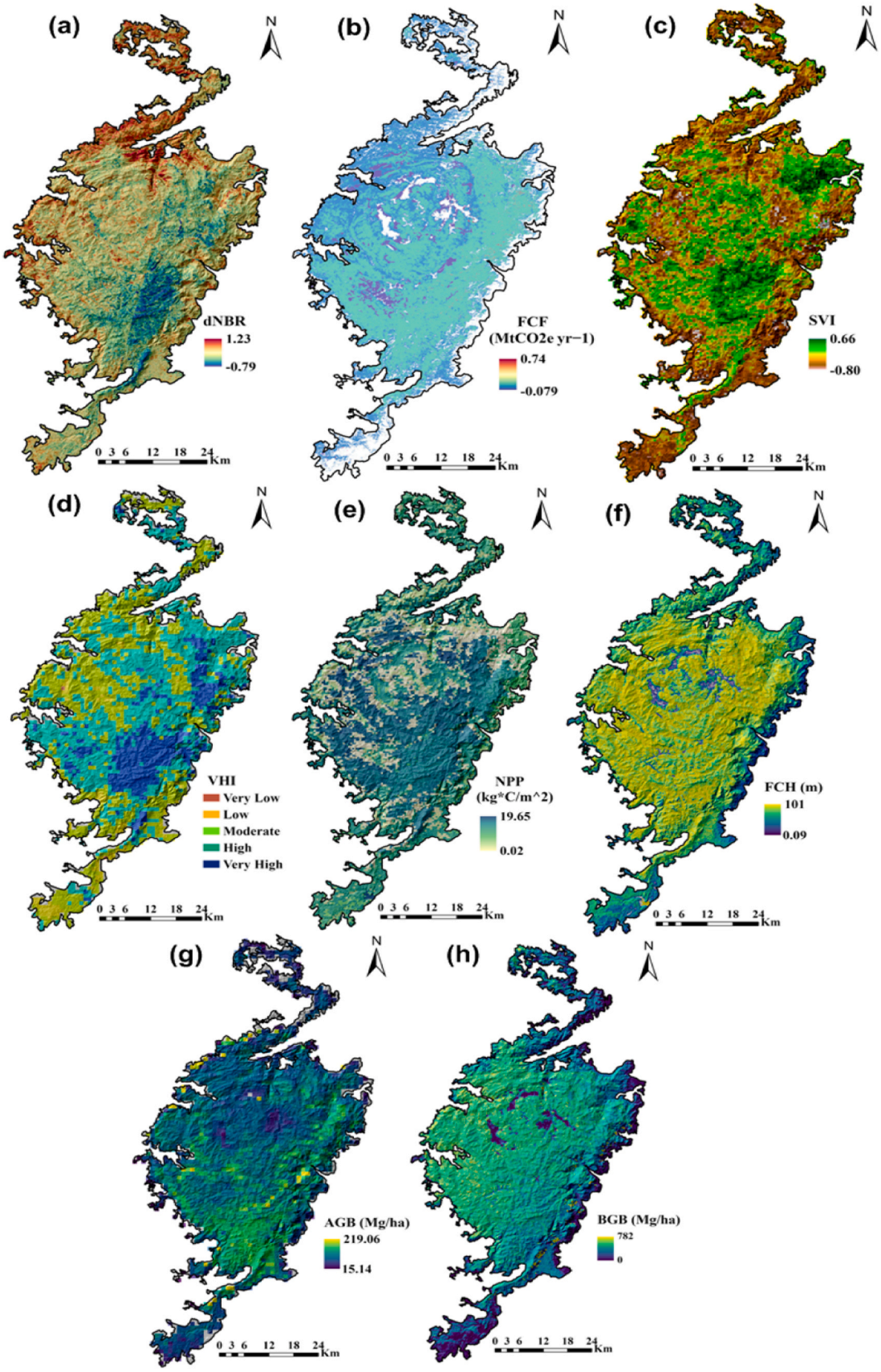

Fig. 5. Forest health factors distribution map, (a) dNBR, (b) FCF, (c) SVI, (d) VHI, (e) NPP, (f) FCH, (g) AGB, and (h) BGB.

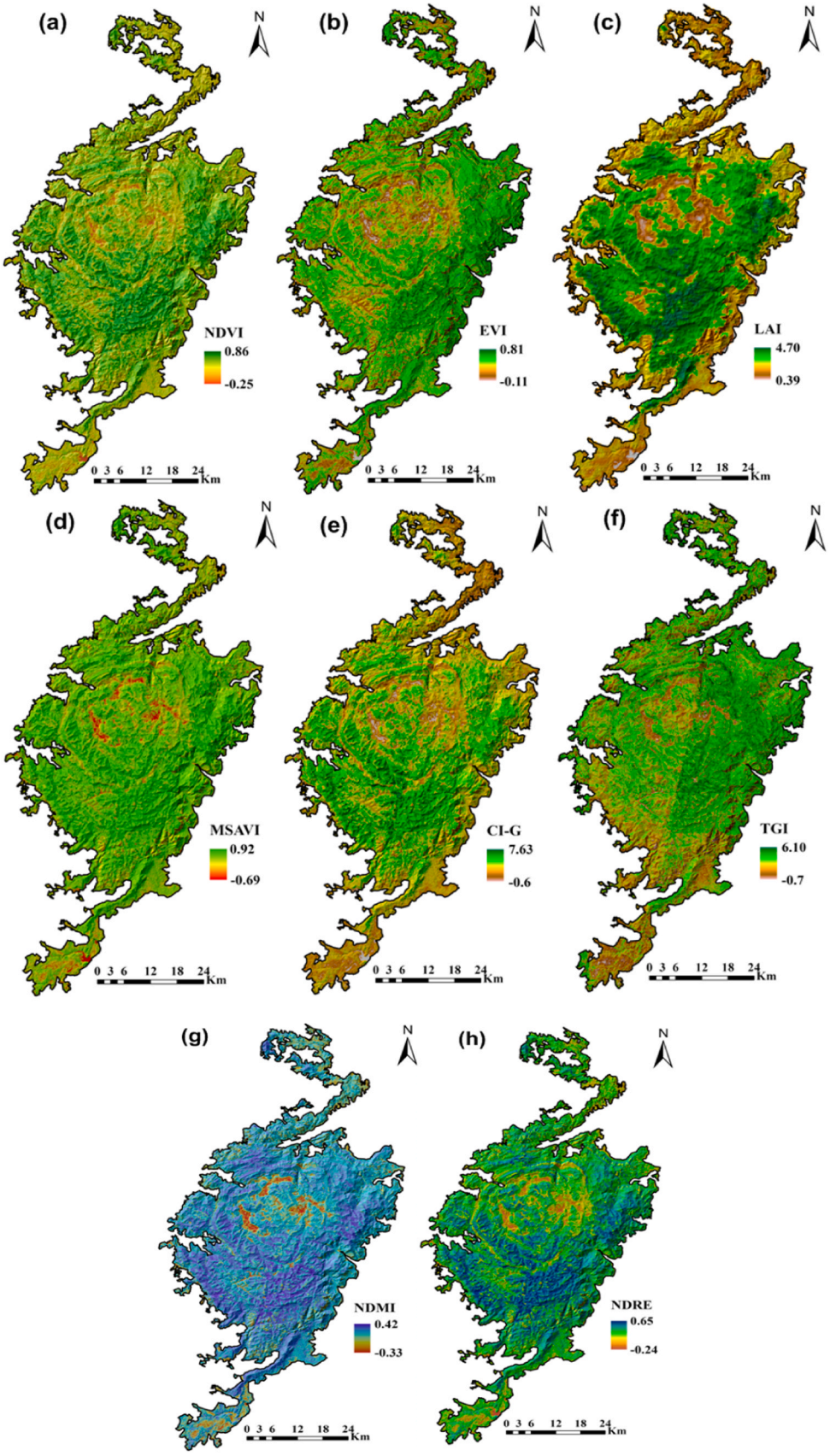

Fig. 6. Vegetation indices maps, (a) NDVI, (b) EVI, (c) LAI, (d) MSAVI, (e) CI-G, (f) TGI, (g) NDMI, and (h) NDRE.

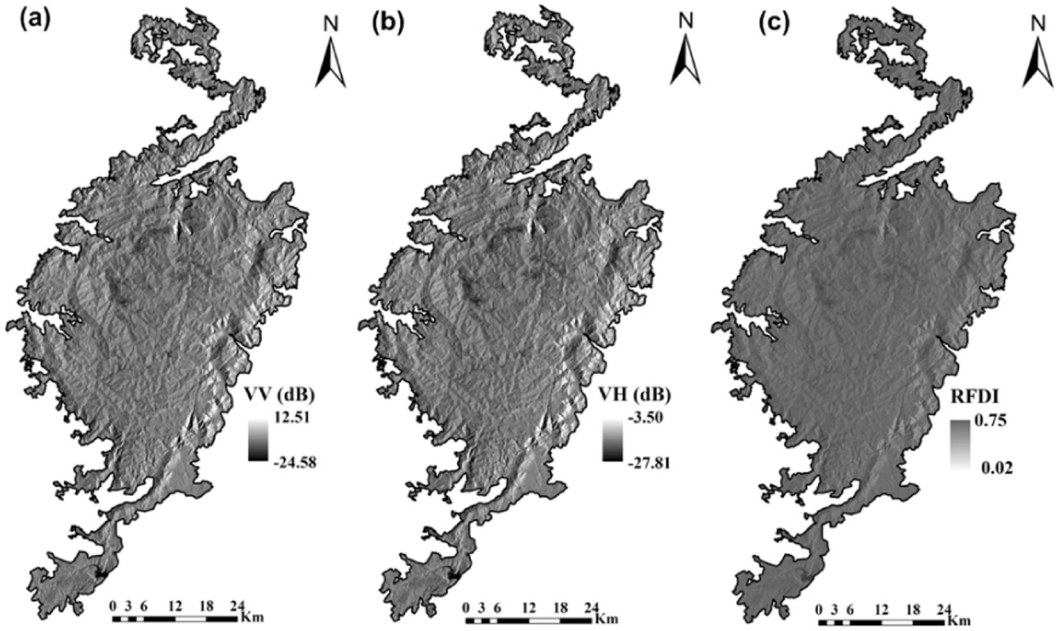

Fig. 7. Radar sat feature maps, (a) VV, (b) VH, and (c) RFDI.

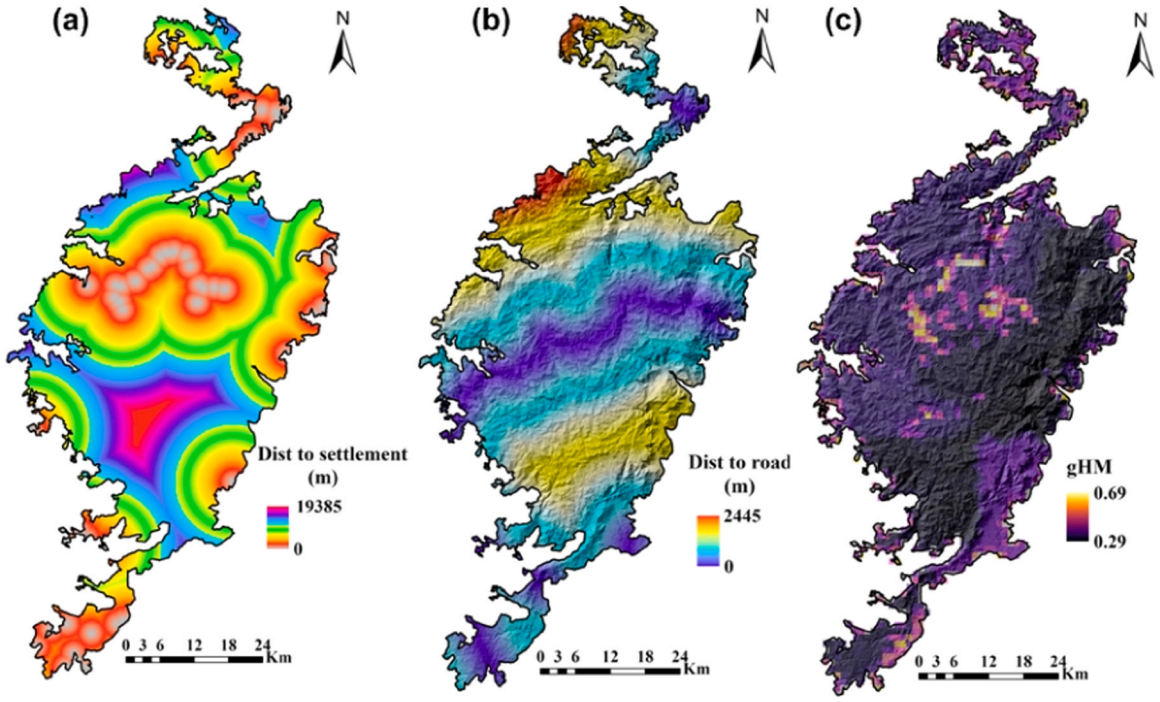

Fig. 8. Anthropogenic interfaces factors, (a) distance to settlement, (b) distance to road (c) gHM.

guide for the search engine to identify the most effective solutions. In addition, the OPF takes into account the various optimization parameters for support vector machines and random forests (Papa et al., 2011). Employing GBS, we determined the optimal *ntree* to be 547 (Supplementary Fig. 1).

2.4.2.6. AdaBag. The AdaBag algorithm is used in machine learning to boost weak-level learners and produce an aggregated model with better precision (Zhu et al., 2009). Weak learners are defined by either being better than random guesses or having poor performance. With the help of this algorithm, the classifiers can be upgraded and produce the best possible final product. It uses the Adaboost.M1 algorithm by Schapire and Freund and the Bagging algorithm by Breiman as its classifiers (Freund, 1996). The current study used the AdaBag algorithm with the subsequent fitting parameters (mfinal =10, coeflearn ="Freund", maxdepth =5, minsplit =1, and cp =−1).

2.4.2.7. Extreme Gradient Boosting (XGBTree). XGBoost is a widely used method to train the model and predict the conditions for the testing sets (Hanberry et al., 2020). The XGBoost algorithm combines the strength of gradient boosting with weak learner predictions to produce more accurate predictions. It is a flexible algorithm that can be used for various

applications namely forest fire, flood mapping, landslide, mapping etc. The main advantage of this method is that it can solve classification and regression problems. The current study optimized the best parameters of the XGBTree asmax_depth= 2, eta= 1, nthread = 2, nfold = 5, nrounds = 200, and lambda = 0.0005 (Supplementary Fig. 1).

2.4.2.8. Gradient Boosting Machine (GBM). GBM is an ensemble ML algorithm that takes into account the sequential models in data space and partitions them into sub-regions to improve the accuracy of the response variable estimate. It also tries to minimize the loss function between the parent nodes (Lee et al., 2019). This method tends to be more robust as it updates the weights according to gradients, which are not sensitive to outlier values. In this study, the tune for gbmGrid, and ROC metric utilized the GBM model efficiency.

2.4.2.9. Grey Wolf Optimization (RF-GWO). The GWO is a novel population-based and heuristic optimization method that creates a pyramid with the most dominant wolf in the hierarchy in lower cases (Mirjalili et al., 2014). The GWO algorithm is suitable for hunting, attacking, and encircling predators. It converges faster and has evolutionary programming compared to swarm intelligence. With only a few parameters, it has a very easy implementation. The GWO algorithm was used for a research project on forest fires (Bui et al., 2019). It randomly places search operators and hunters in a certain region and their fitness and position information are continuously updated. The algorithm's most optimal solution is to find the top wolf. The current study RF optimized the GWO algorithm for mapping FFS in the STR region. Employing GWO, we determined the optimal *ntree* to be 506 (Supplementary Fig. 1).

2.4.2.10. Particle Swarm Optimization (RF-PSO). The PSO algorithm was presented by Eberhart and Kennedy in 1995. It is another meta-heuristic algorithm that approximates the treatment of aquatic animals. The particles are examined in the PSO algorithm and are looked for the most suitable solutions. These are evaluated using their velocity and position, and the former determines the magnitude and direction of the particle's movement while the latter determines its quality (Asadi et al., 2021). The samples and training features of an RF are generated using a bootstrap method. The number of sets that are used is also decided randomly. In our study, employing PSO, we determined the optimal *ntree* to be 497 (Supplementary Fig. 1).

2.4.3. Future FFS

The current study showed the future forest fire trend analysis (2022–2100) using the CMIP6 (EC-Earth3) shared socio-economic pathway (ssp245 and ssp585) dataset with the MIROC6 model (Thrasher et al., 2012). The GEE cloud is used for the slope of linear regression (SLR) methods of spatial-temporal mapping for future purposes. The current study considered five factors (i.e., precipitation, solar radiation, wind speed, minimum temperature and maximum temperature) for future FFS mapping within both scenarios.

2.5. Validation analysis

For FFS mapping validation, the current study compared 10 different ML classification results. The 10-fold cross-validation was applied with different statistical elements accuracy, kappa coefficient, sensitivity, specificity, positive predictive values (PPV), and negative predictive values (NPV) to evaluate the model's performance (Naderpour et al., 2021):

$$Accuracy = \frac{TP + TN}{TP + TN + FP + FN} \quad (1)$$

$$Kappa\ \ coefficient = \frac{P_{obs} - P_{\exp}}{1 - P_{\exp}} \quad (2)$$

$$Sensitivity = \frac{TP}{TP + FN} \quad (3)$$

$$Specificity = \frac{TN}{TN + FP} \quad (4)$$

$$PPV = \frac{TP}{TP + FP} \quad (5)$$

$$NPV = \frac{TN}{TN + FN} \quad (6)$$

where, *TP*, *TN*, *FP*, and *FN*, respectively, are true positive, true negative, false positive and false positive, and false negative, while P_{obs} and $P_{\exp}$ are observed and predicted fire, respectively,.

2.6. Boruta sensitivity and SHapley Additive exPlanations (SHAP) analysis

This study delves into the application of the Boruta wrapper algorithm to analyze the sensitivity of factors associated with forest fire ignition (Chen et al., 2022). Using the RF model, the Boruta method proves effective in predicting FFS mapping. Additionally, the SHAP method, widely recognized for assessing prediction algorithms, was employed to provide clear and interpretable explanations for the model's outputs (Chen et al., 2021).

3. Results

3.1. OLS and multi-collinearity evaluation

To identify optimal features for FFS models, an analysis of the significance of independent variables was conducted through Pearson correlation, OLS, and multi-collinearity. The results of the Pearson correlation in Fig. 9 indicated a robust negative relationship between forest fire probability and factors such as humidity, precipitation, TWI, LAI, EVI, AET, distance to road and settlement. Additionally, an inverse correlation was observed with aspect, solar radiation, distance to river, Tmax, Tmin, TVDI, and PDSI variables (see Fig. 9). OLS analysis highlighted that dNBR, distance to settlement, Tmax, NDVI, EVI, and TGI were highly significant (> 99%) contributors to forest fire occurrence. The coefficients ranged from − 5.50 (NDVI) to 7.22 (MSAVI), with R^2 ~0.80 and an F statistic ~21.92 indicating a strong concordance among parameters (see Table 2). Multicollinearity tests, conducted via VIF, revealed no issues among the factors influencing forest fire ignition. The maximum and minimum VIF were observed for VV (1.5) and TGI (7.37), respectively, both well below the 10 cutoff limit (see Table 1).

3.2. Spatial FFS prediction

The FFS was classified into five categories using the natural break procedure in ArcGIS: very low, low, moderate, high, and very high. The distribution of FFS classes was obtained from the predicted ML models (Table 2). According to the RF-GA model, the susceptibility classes covered 12.81% (very high), 20.51% (high), 22.88% (moderate), 20.42% (low), and 23.38% (very low) of the total area (Fig. 10a). The nnet model indicated that approximately 33.02% of the study area had high to very high susceptibility, while 43.73% was classified as low or very low susceptibility to forest fires. In the RF-DEA model outcomes, the very low, low, and moderate susceptibility classes covered 23.48%, 20.42%, and 22.93% of the study area, respectively. The high and very high classes occupied 20.46% and 12.72% of the area, respectively. The RF-GBS model allocated the largest extent to the very high fire-susceptible zone (12.15%) and the very low fire-susceptible zone (24.32%) (Fig. 10 (d)). The 10-fold cross-validation RF model predicted that the moderate, low, and very low classes covered 23.89%, 21%, and 23.11%

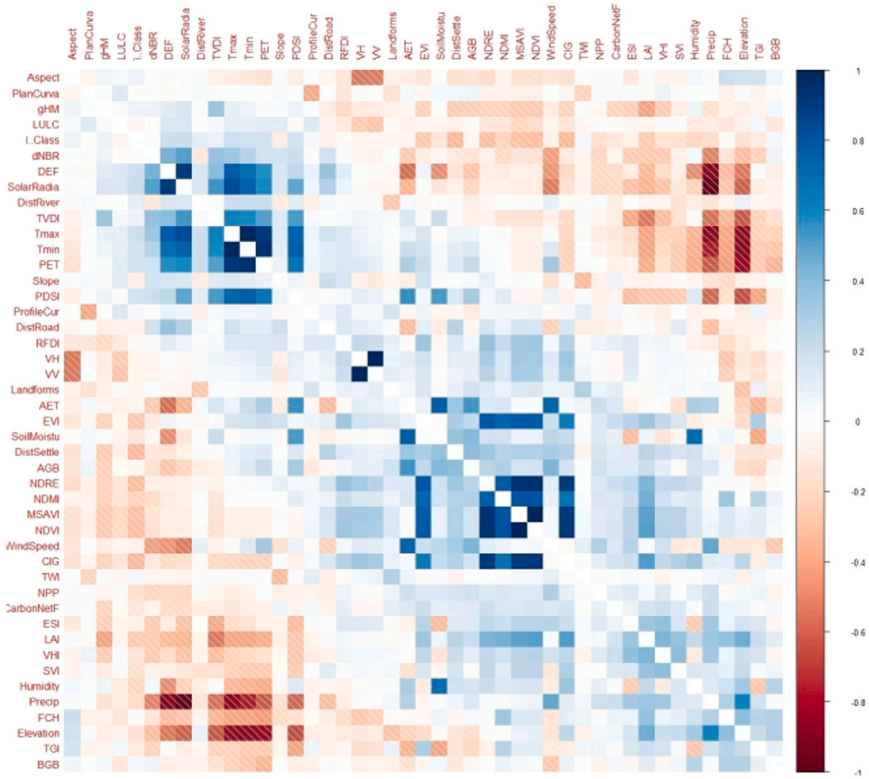

Fig. 9. Pearson correlation matrix for forest fire ignition factors.

of the research area, while high and very high classes were estimated to cover 20.12% and 11.88% of the area, respectively. In the case of the AdaBag model, the very low, low, moderate, high, and very high classes covered 20.01%, 18.48%, 22.71%, 23.20%, and 15.60% of the land area, respectively. The cumulative areal coverage of the moderate, high, and very high susceptibility classes in the XGBTree model accounted for 42.6% of the study area, compared to 47.42% and 57.74% with the GBM and RF-GWO models, respectively (Fig. 10 (g)). Finally, the RF-PSO model designated approximately 12.89% as very high, 24.40% as high, 25.03% as moderate, 19.10% as low, and 18.57% as very low fire susceptibility (Fig. 10 (j)).

The susceptibility clusters exhibited nearly similar patterns for the ML models. For instance, the high and very high susceptibility groups were prominent in the north and the edges of the south of the study area, whereas the very low susceptibility cluster was occupied in the central zone.

3.3. Validation

As can be seen from Table 3 and Fig. 11, the evaluation of various hybrid/single ML models in this study revealed their remarkable ability to identify areas prone to forest fires in STR. Overall, the RF-PSO model had the best performance, with an AUC of 0.89, showcasing its exceptional ability to accurately predict fire-prone areas. The nnet model closely followed, demonstrating a remarkable AUC of 0.88. The remaining models also exhibited commendable performance, with AUC values ranging from 0.84 to 0.87.

Notably, the RF-PSO and nnet models displayed a relatively balanced trade-off between sensitivity and specificity, indicating their ability to accurately identify fire-prone areas while also pinpointing non-fire-prone regions with equal precision. This balanced performance was further supported by their high Kappa values, reinforcing their overall effectiveness in forest fire susceptibility prediction in the STR.

3.4. Future FFS mapping

After analyzing the final validation results, we determined that the RF-PSO model was the best choice for generating the future FFS map. Linear trends were applied to predict future FFS under two CMIP6 climate change scenarios (ssp245 and ssp585 for 2022–2100), as depicted in Fig. 12 (a) and (b). For the ssp245 scenario (2022–2100), the resulting map showed areas classified as very low susceptibility (37.69% of the total area), low (20.68%), moderate (15.18%), high (12.56%), and very high (13.89%). Under the ssp585 scenario (2022–2100), 13.14% of the total area was classified as very highly susceptible, 14.15% as high, 15.79% as moderate, 20.53% as low, and 36.38% as very low susceptible zones (Supplementary Table 3). On average, approximately 26.45% to 27.29% of the STR area exhibited high to very high susceptibility zones, warranting immediate measures for future forest fire monitoring. The northern and southern outskirts of STR showed particularly high susceptibility, while the central zone was classified as a low to very low susceptibility zone.

The forest fire probability under two future climate change scenarios: SSP245 and SSP585, was assessed using the RF-PSO model. The results are summarized in Table 4 and Fig. 13. The RF-PSO model demonstrated a commendable AUC value of 0.86, indicating robust predictive accuracy above 0.81 (see Fig. 13 and Table 4). The kappa value indicates moderate to strong agreement between the model's predictions and the actual FFS values for both SSP245 and SSP585. Overall, the RF-PSO model is a good predictor of future FFS values for both SSP245 and SSP585 as it had reasonable performance across considered metrics. This is properly related to its ensemble structure, combining RF and PSO, enhancing its ability to capture complex relationships between forest fire risk factors and FFS values.

3.5. Boruta Sensitivity and SHAP Evaluation

Forest fire feature plot showed that all 29 factors had significant contributions to monitoring forest fire in the STR region (Fig. 14).

Table1
OLS and VIF analysis results for fog water potentiality parameters.

Features	Coef.	Std err.	t	P > |t|	VIF
NDRE	-0.03	1.87	-0.02	0.99	3.57
NDVI	-5.50	8.41	-0.65	0.51	2.38
NPP	-0.02	0.01	-1.55	0.12	1.31
PDSI	0.06	0.02	2.72	0.01 * *	3.49
PET	0.01	0.00	1.87	0.06	2.83
PlanCurva	0.04	0.07	0.63	0.53	1.42
Precipitation	0.01	0.02	0.47	0.64	2.88
ProfileCur	0.05	0.07	0.83	0.41	1.44
RFDI	0.70	0.31	2.28	0.02 *	1.46
Slope	-0.01	0.00	-1.55	0.12	1.70
SoilMoisture	0.00	0.00	1.80	0.07	4.43
SolarRadiation	0.01	0.01	1.47	0.14	3.49
SVI	-0.01	0.02	-0.69	0.49	1.52
TGI	0.00	0.00	-3.22	0.00 * **	7.37
Tmax	-0.30	0.11	-2.82	0.01 * *	4.76
Tmin	0.17	0.09	1.78	0.08	5.55
TVDI	-0.32	0.43	-0.74	0.46	3.39
TWI	0.00	0.01	0.34	0.74	1.39
VH	0.03	0.10	0.25	0.80	4.43
VHI	0.03	0.04	0.84	0.40	1.71
VV	-0.03	0.09	-0.31	0.76	1.15
WindSpeed	-0.03	0.03	-1.19	0.24	1.97
AET	0.02	0.02	1.09	0.28	5.39
AGB	0.00	0.00	2.35	0.02 *	2.07
Aspect	0.01	0.01	1.39	0.17	1.54
BGB	0.00	0.00	0.93	0.35	1.43
CarbonNetFlux	0.00	0.00	-0.23	0.82	1.39
CIG	-0.24	0.14	-1.75	0.08	5.85
DEF	0.04	0.02	3.00	0.00 * **	4.56
DistRiver	0.00	0.00	1.46	0.15	1.71
DistRoad	-0.61	0.63	-0.97	0.33	2.74
DistSettle	0.00	0.00	-4.03	0.00 * **	2.55
dNBR	0.00	0.00	-4.11	0.00 * **	2.55
Elevation	0.00	0.00	-0.93	0.35	3.67
ESI	0.00	0.00	-0.56	0.58	1.94
EVI	0.85	1.09	0.78	0.43	4.54
FCH	0.01	0.01	0.56	0.57	2.44
gHM	-0.48	0.77	-0.63	0.53	1.73
Humidity	-0.03	0.02	-1.68	0.09	6.60
LAI	-0.03	0.04	-0.88	0.38	3.09
Landforms	0.00	0.01	-0.39	0.70	2.00
LULC	-0.03	0.01	-2.20	0.03 *	1.89
MSAVI	7.22	10.06	0.72	0.47	6.85
NDMI	0.74	0.84	0.89	0.37	6.47
R^2 (0.80)	F statistic (21.92),	Prob>chi^2 (0.001)	Durbin Watson (0.660)		

β ~Coefficient; t~t test std err~ Standard error, Robust standard errors~ *p < 0.05, * *p < 0.01, and, * **p < 0.001,F~ Statistical, R^2~ Linear regression.

Table 2
Areal coverage of forest fire susceptible zones in STR region.

Models	Cover	Very Low	Low	Moderate	High	Very High
RF-GA	km^2	472.55	412.74	462.42	414.50	259.00
	%	23.38	20.42	22.88	20.51	12.81
nnet	km^2	473.12	410.61	470.04	415.99	251.42
	%	23.41	20.32	23.26	20.58	12.44
RF-DEA	km^2	474.55	412.74	463.42	413.50	257.00
	%	23.48	20.42	22.93	20.46	12.72
RF-GBS	km^2	491.54	422.41	454.72	406.85	245.67
	%	24.32	20.90	22.50	20.13	12.15
RF	km^2	467.10	424.41	482.82	406.74	240.14
	%	23.11	21.00	23.89	20.12	11.88
AdaBag	km^2	404.41	373.52	459.10	468.87	315.30
	%	20.01	18.48	22.71	23.20	15.60
XGBTree	km^2	881.00	279.11	218.73	237.24	405.12
	%	43.59	13.81	10.82	11.74	20.04
GBM	km^2	649.04	413.65	336.95	313.36	308.19
	%	32.11	20.47	16.67	15.50	15.25
RF-GWO	km^2	420.37	433.66	462.14	433.59	271.44
	%	20.80	21.46	22.86	21.45	13.43
RF-PSO	km^2	375.41	385.97	505.93	493.27	260.62
	%	18.57	19.10	25.03	24.40	12.89

Additionally, the ranking of effective factors for the forest fire ignition estimated with the highest value to AET (14), followed by relative humidity (12.31), distance to settlement (11.97), PET (11.96), solar radiation (10.24), LAI (9.71), DEF (9.60), DEF (5.09), MSAVI (9.33), NDVI (9.20), CIG (8.83), Wind speed (8.66), Tmin (8.24), NDRE (8.05), distance to road (7.62), Tmax (7.50), EVI (7.36), PDSI (7.32), NPP (7.23), gHM (6.41), Soil moisture (5.99), dNBR (5.95), Precipitation (5.92), SVI (5.24), AGB (4.56), NDMI (4.18), Elevation (3.99), TGI (3.70), Carbon Net fluxes (3.43), and TVDI (3.41) (Supplementary Table 4). However, VHI was a tentative factor while the Slope, ESI, BGB, distance to river, FCH, RFDI, VH, Aspect, VV, Plan curvature, Profile curvature, Landforms, LULC and TWI are less important among all ignition factors.

The SHAP technique provides a comprehensive overview of the various features used in the prediction analysis. However, due to the unique results of each feature, there is potential for more complex visualizations.

Based on the decision plot (Fig. 15 (b)), the forest fire score showed a satisfactory increase when factors moved towards the right, while it was negatively affected by factors moving towards the left. Similar to the summary plot (Fig. 15 (a)), the decision plot offers a broad overview of the predicted outcome. Factors are plotted on the Y-axis, and their SHAP values (indicating impact on the model output) are shown on the X-axis. This helps us understand how distance to road, distance to settlement,

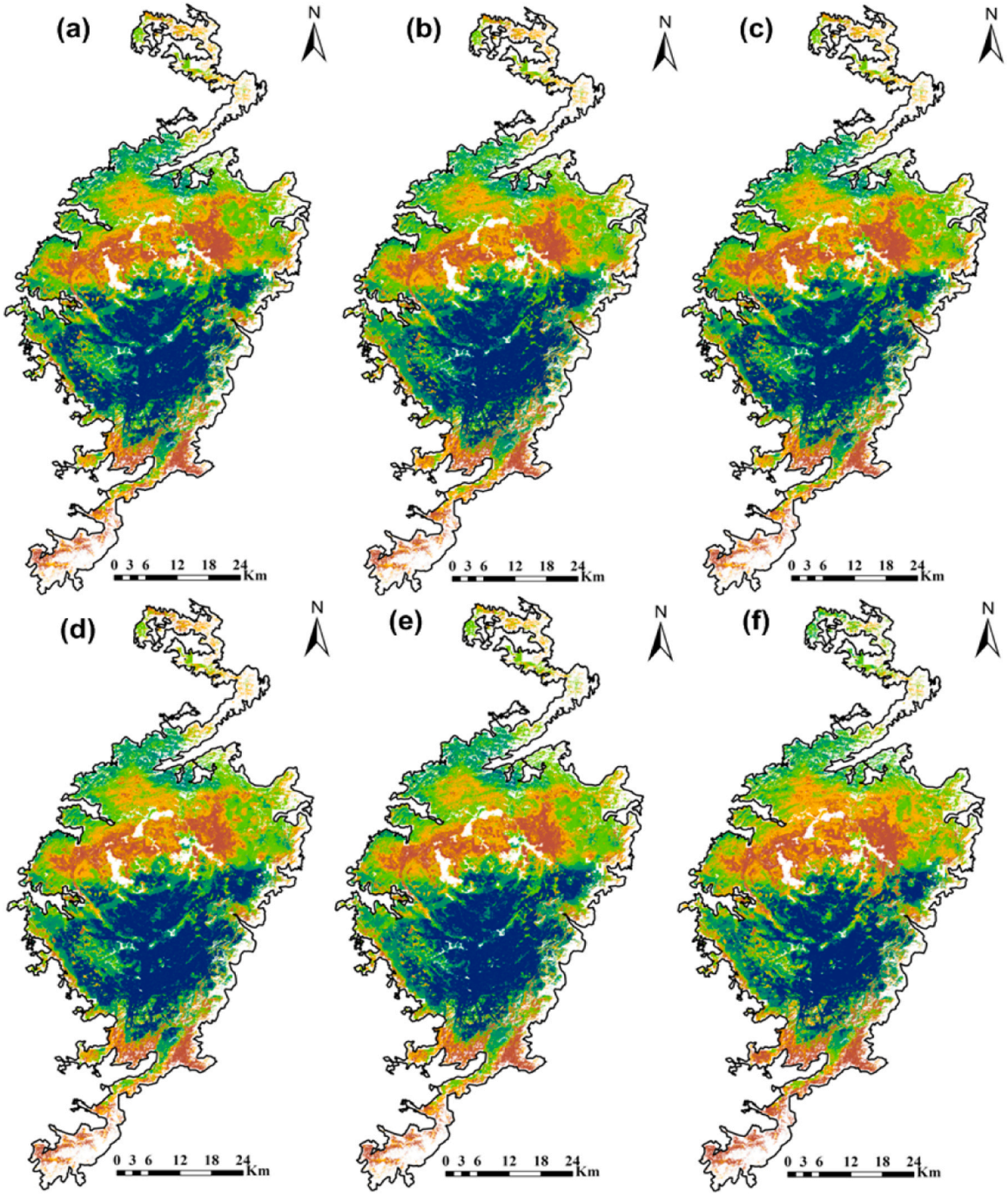

Fig. 10. Prediction of forest fires susceptibility maps (a) RF-GA, (b) nnet, (c) RF-DEA, (d) RF-GBS, (e) RF, (f) AdaBag, (g)XGBTree, (h) GBM, (i) RF-GWO, and (j) RF-PSO.

dNBR, slope, and humidity values exerted the most significant influence on the prediction. High values of PET, AET, and humidity were associated with unfavorable outcomes. Additionally, wind speed and response factor showed favorable correlations.

The SHAP explanation, illustrated in a forced plot, reveals how different features interact to increase the model's output from its base value to its predicted one (see Fig. 15 (c)). For instance, the optimization of factors in predicting forest fires was 0.60, whereas the baseline value stood at 0.5387 (see Fig. 15 (c)). The final output prediction can be enhanced by relatively high LAI, solar radiation, and wind speed, as well as low precipitation, distance to settlement, and distance to road. Conversely, the forecast accuracy may be diminished by relatively high humidity.

3.6. Forest fire susceptibility map rationality

The rationality of the FFS maps was assessed using the results in Table 2, Fig. 14 & 15. Drawing inspiration from studies (Ozalp et al., 2023; Guo et al., 2021; Shi and Zhang, 2023), the rationality of the susceptibility map can be assessed in two aspects: (I) Forest fires should be positioned in areas of high susceptibility, considering various geo-environmental ignition factors (e.g., climate, topography,

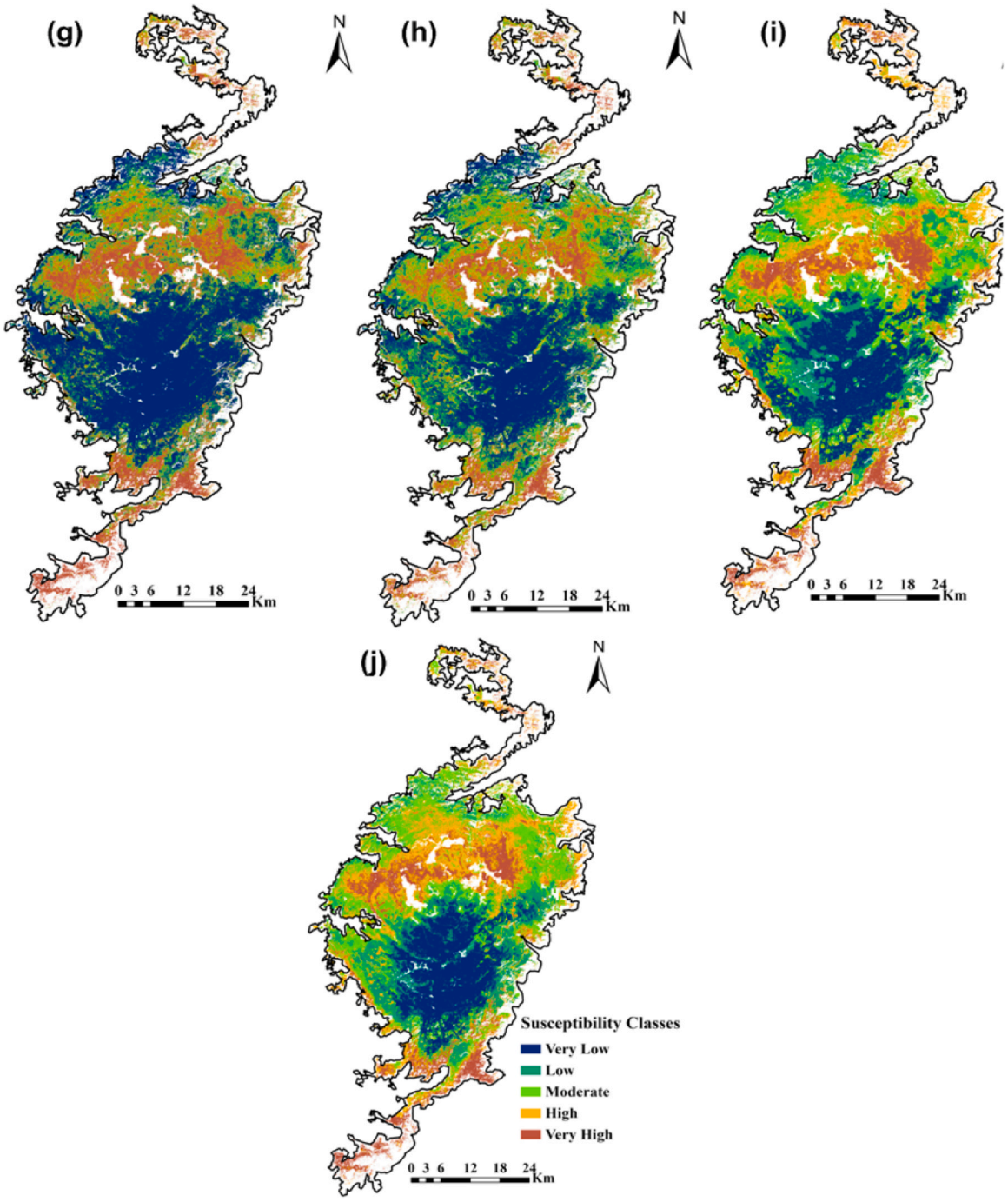

Fig. 10. (*continued*).

Table 3
Summary of the ML models performance for FFS estimation.

Model	Accuracy	Kappa	Sensitivity	Specificity	PPV	NPV	AUC
RF-GA	0.79	0.58	0.81	0.76	0.77	0.80	0.87
nnet	0.82	0.64	0.88	0.76	0.79	0.87	0.88
RF-DEA	0.81	0.61	0.88	0.73	0.76	0.86	0.88
RF-GBS	0.79	0.58	0.85	0.73	0.76	0.83	0.87
RF	0.76	0.52	0.81	0.71	0.76	0.77	0.88
AdaBag	0.77	0.54	0.92	0.63	0.71	0.88	0.85
XGBTree	0.75	0.51	0.80	0.71	0.73	0.78	0.84
GBM	0.79	0.58	0.86	0.71	0.75	0.84	0.86
RF-GWO	0.81	0.62	0.89	0.73	0.79	0.85	0.88
RF-PSO	0.81	0.63	0.85	0.78	0.79	0.84	0.89

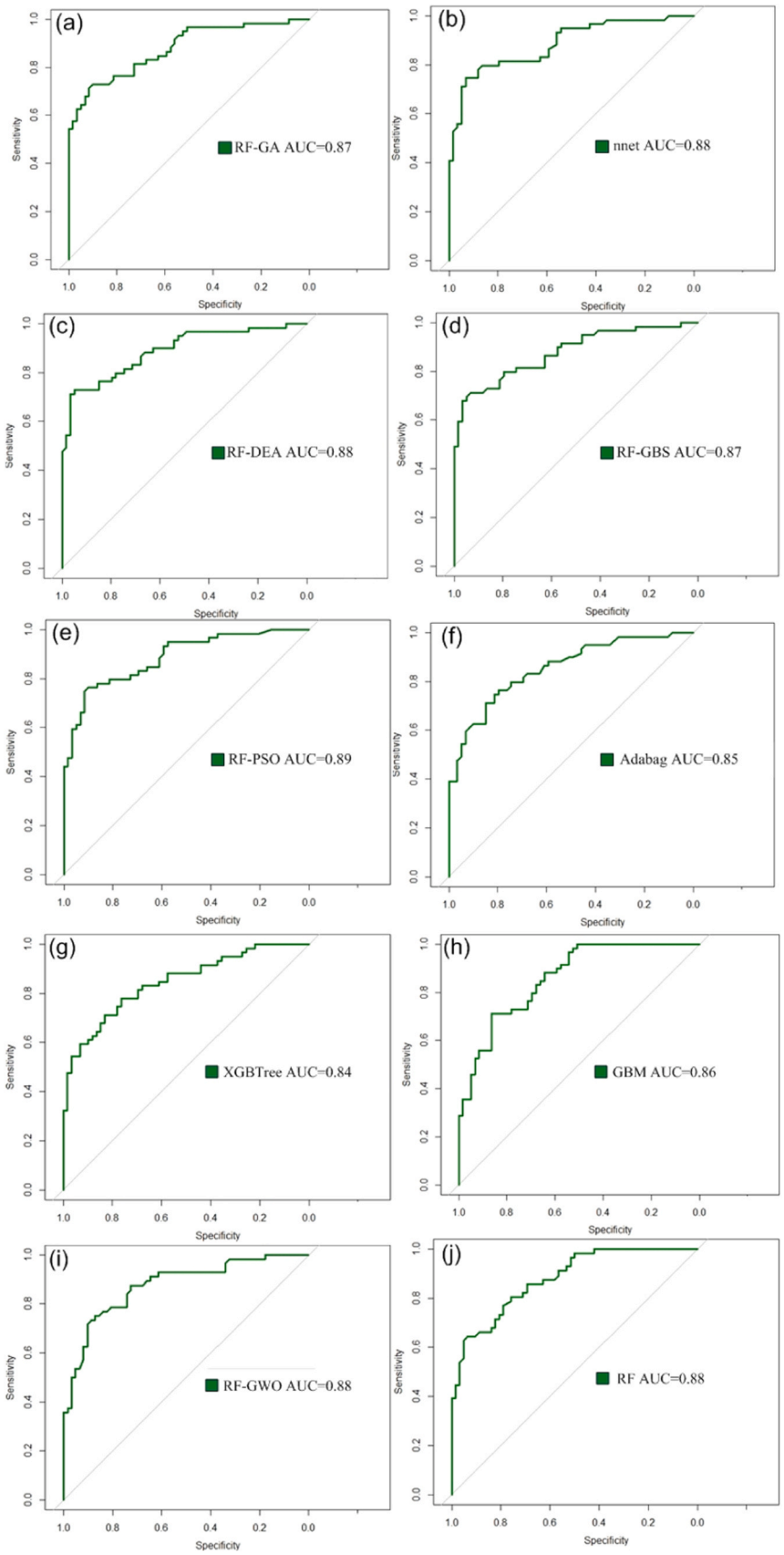

Fig. 11. AUROC for fire susceptibility evaluation.

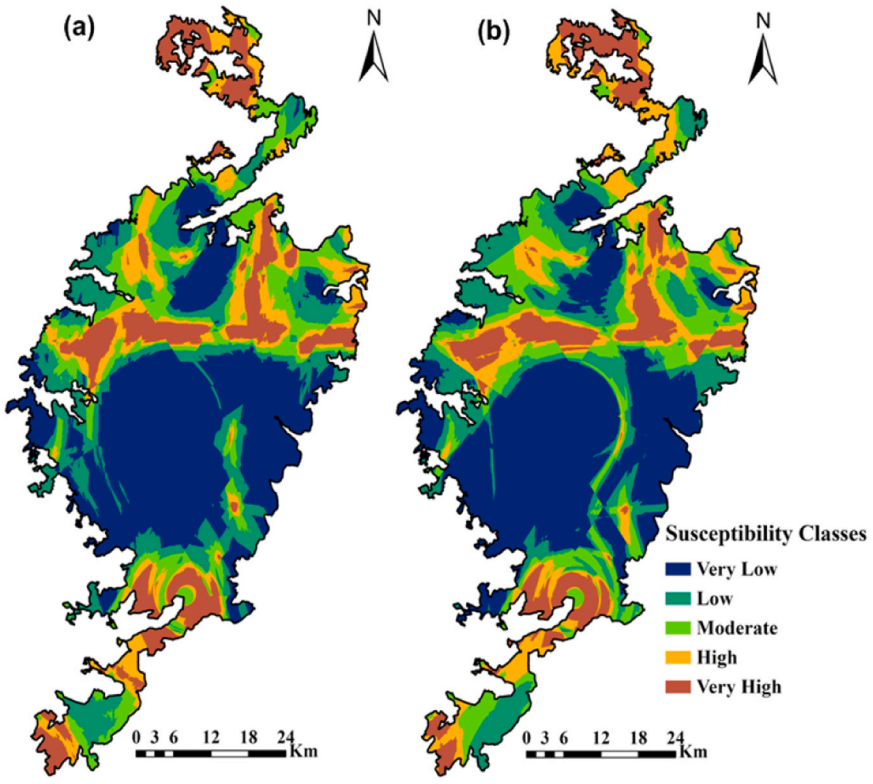

Fig. 12. Prediction of future FFS maps based on CMIP6 (2022–2100), (a) ss245 and (b) ssp585.

Table 4
Future FFS estimation through RF-PSO model.

Metrics	ssp245	ssp585
Accuracy	0.81	0.83
Kappa	0.61	0.65
Sensitivity	0.80	0.82
Specificity	0.81	0.83
PPV	0.81	0.82
NPV	0.80	0.83
AUC	0.86	0.86

vegetation, and anthropogenic interfaces); and (II) areas of very high FFS in the susceptibility map must be minimized.

The results of the studies revealed a consistent trend in the FFS models generated by hybrid/single ML models. As the number of forest fire incidents increased, the frequency of these events also increased, with the highest incidence rate found in the models that were most vulnerable to forest fires. The results reported in Table 2 established that the formed FFS maps were reasonable, showing an increasing ratio of forest fire occurrence from areas with very low FFS to very high FFS. Overall, FFS maps derived from the RF-PSO and nnet models appeared to be more sensible than those resulting from other considered models.

Concerning the first criterion, the RF-PSO model (AUC of 0.89) demonstrated high sensitivity to FFS analysis. The second criterion, which emphasized terrain and anthropogenic factors as crucial ignition capability indicators for producing FFS maps (Fig. 14 & 15), further supported the effectiveness of our results. Both criteria evaluations indicate that our findings are applicable, effective, reasonable, and rational for the study area.

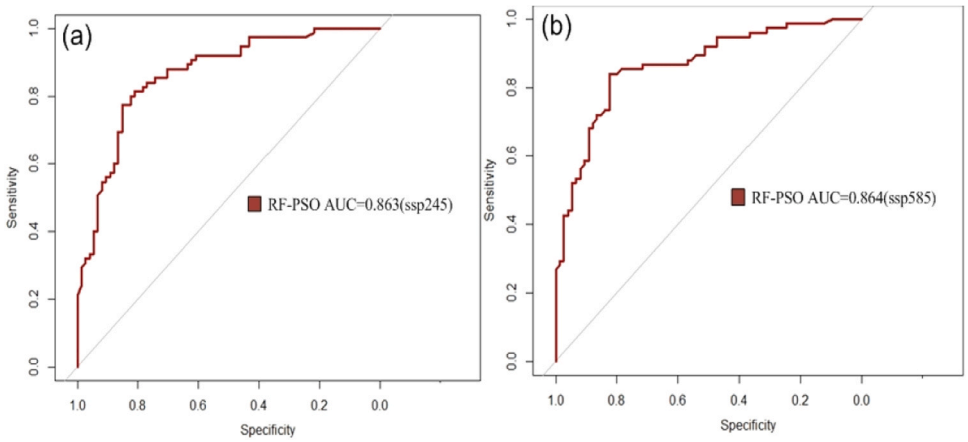

Fig. 13. CMIP6 based AUROC for future FFS evaluation.

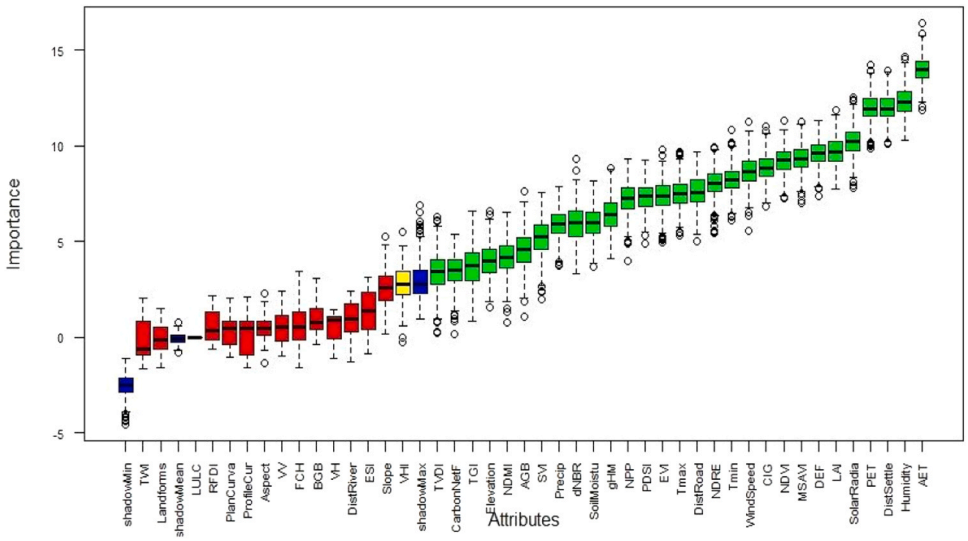

Fig. 14. Boruta factor sensitivity analysis for FFS evaluation.

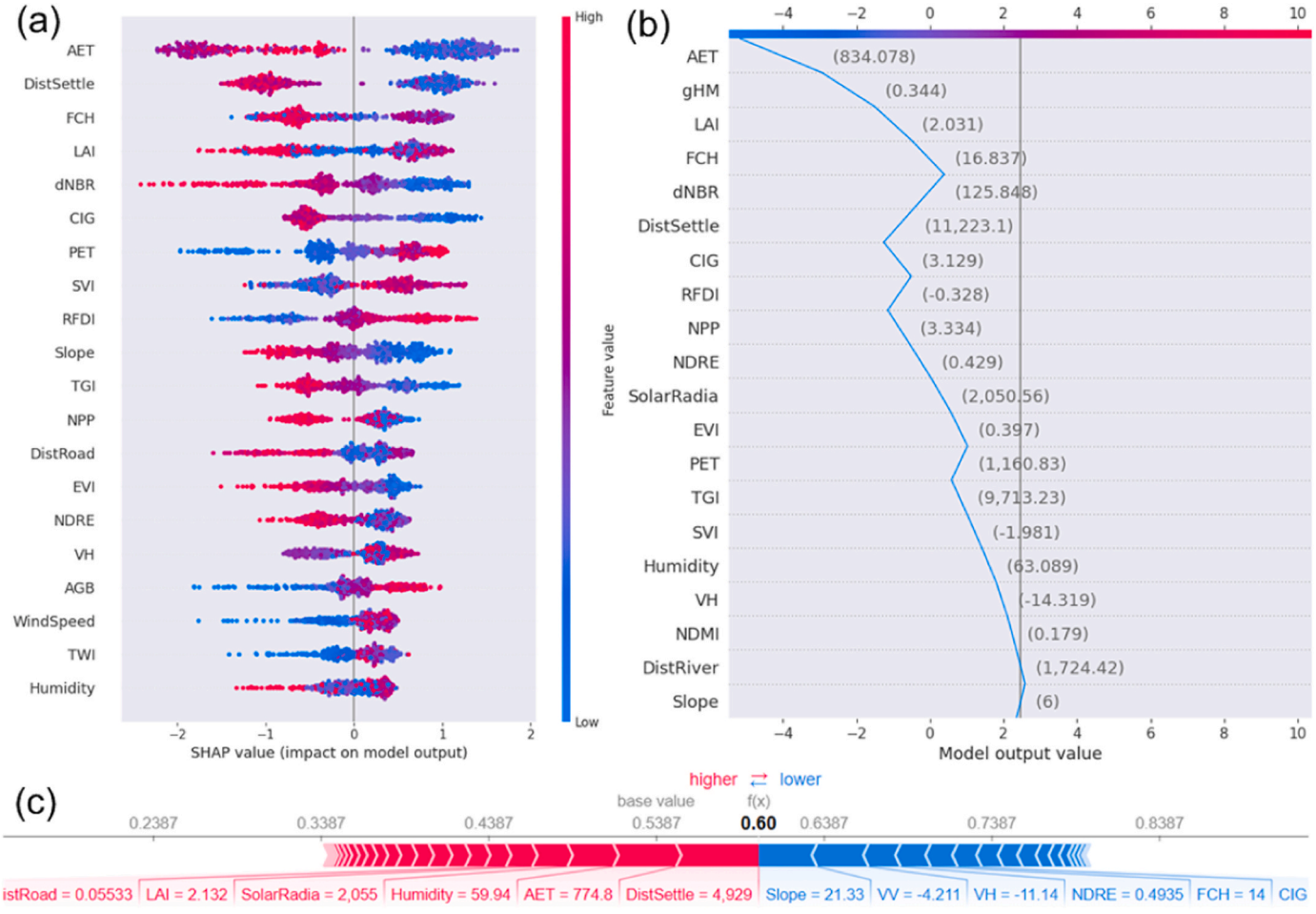

Fig. 15. SHAP explanation for FFS evaluation, (a) summary plot, (b) decision plot (c) force plot.

4. Discussion

The use of ML algorithms has become a popular approach in wildfire susceptibility mapping (Shmuel et al., 2022). In this study, the prediction capabilities of metaheuristic ML classifiers (RF-GA, nnet, RF-DEA, RF-GBS, RF, AdaBag, XGBTree, GBM, RF-GWO, and RF-PSO) were compared to generate the FFS zone in the selected STR region. The RF-PSO and nnet algorithms performed better than the other classifiers in several performance metrics. Similarly, other researchers found the same results likely the RF and nnet models perform admirably best in wildfire susceptibility studies (Ghorbanzadeh et al., 2019, Shmuel et al., 2022). The SHAP and Boruta algorithms were able to identify the most

effective ignition factors that can improve wildfire susceptibility mapping. In the STR analysis, distances to the road, distance to settlement, AET, windspeed, temperature and humidity were identified as the most predictive factors. The presence of anthropogenic interfaces has been identified as a significant factor that contributes to the spread and formation of wildfires in natural regions (Bowman et al., 2018). Human intactness is the key role of forestland fires, whether fortuitously or purposely (Flannigan et al., 2000). It is assumed that the adjacent settlements and roads are good proxies of forest fire occurrence (Zhang et al., 2021). Zumbrunnen et al. (2012) indicated that rural villages can play a key role in wildfire development.

Topographic distribution can also influence the ignition pattern of fire, accessibility to people, and the flammability of a forest. Moreover, the topographic variation might influence the local climate and the distribution of vegetation. The slopes can help limit the risk of wildfires by restricting their accessibility. The elevation range, aspect direction, slope angle, curvature geometry and landform relief patterns affect fire occurrences in any geographical location (Zhao et al., 2022). The SAR backscatter also reflects the AGB, forest canopy height and carbon storage density. The pre-fire identification can measure initial fuel accessibility (Li et al., 2019). Meanwhile, dense vegetation ignition is more likely that the wildfire will spread in areas with high fuel loads.

The vegetation indices are also important factors to be considered for determining the likelihood of forest fires. The forest phenology components of the forest health condition are an ideal mechanism for the fire occurrence (Li et al., 2022). The presence of below-ground mass (BGB) and unhealthy vegetation can contribute to the development and spread of wildfires. It can also provide easy access to fuel for fire events due to a higher percentage of dead leaves and branches. A number of studies have shown that the presence of numerous biophysical factors, such as LAI, NPP, ESI, AET, PET, VHI, NDWI, NDMI, SVI and LST, can contribute to the favourable conditions for fuel moisture condition as well as the wildfires suitability (Abdollahi and Pradhan, 2023). The presence of dry biomass also directly affects the fuel availability, fire spread, and fuel ignitability of fuels. It is an important factor that can be used to evaluate the fire risk. It can also determine the degree to which vegetation is dry before and during the fire season. Reducing rainfall can also contribute to the desiccating of forest fuels and drying vegetation. SAR-derived VV, VH and RFDI had the capability to measure the dryness level (Rao et al., 2020).

The climate conditions during the fire season can also affect the development and spread of forest fires. These include the reduction in vapour pressure and rainfall, climate water deficit, wind speed, humidity as well as high temperature, solar radiation, and etc. Wind speed monitors the movement of fire flames and sparks towards fresh vegetation, as well as removing soil surface moisture/soil. The climate variability provides a direction to the fuel characterization process, which includes the moisture content, fuel load, and degradation (Kerr et al., 2018). Eskandari et al. (2020) noted that the distance from drainage, TWI, and soil moisture conditions could help to prevent wildfires from spreading.

Times of India (2021) reported that most of the fire events quickly occurred in the longer dry season (March-May 2021) due to their heavy abundance of tree dead leaves from dry deciduous forests in the STR region. This condition led to rapid expansion and ignition of the fire. High levels of human activity within the transitional and buffer zones are known to increase the fire risk within the area. Although natural causes such as lightning are sometimes the cause of forest fires in the STR, they are mostly human activities that are the culprit. The Indian Express stated that poachers set fires in forested areas for hunting. These small fires could lead to worse fire situations in the future. The wildfire in the STR region usually extends from various areas, such as fringe lands, adjacent to agricultural fields, campfires, picnic spots, hotels, and road junctions. Human activity, particularly livestock overgrazing, is believed to be the main cause of wildfires in this area (Saranya et al., 2014; Modugno et al., 2016). It was reported that between 2004 and 2013, approximately 11.5% to 27.8% of the STR region was affected by wildfires (Saranya et al., 2014).

The climate and weather conditions play a significant role in determining the global to local wildfire regime and distribution of burnable land (Gallo et al., 2023). Climate change is the key factor for the extent of forest fire risk zones as well as the help to identification of fire regimes cluster (Halofsky et al., 2020).

It is also important to take the necessary fire precautions to reduce the risk of wildfires. Some sources claimed that human error, specifically the actions of travellers and tourists, caused the forest fires. In 2018, the Government of India established a national action plan to prevent forest fires through joint forest management and community development awareness. It aims to empower communities around forests and motivate them to work with the authorities. Early warning systems are also being considered as a strategy to prevent forest fires from occurring in the study area (Nuryanto et al., 2021). The government should create instruments that will allow decision-making regarding the activities within the forest. These include establishing monitoring stations, deploying firefighting equipment and personnel, chemicals, fire distinguishers and patrolling forest buffers. The forest department should also provide emergency forest fire services. Numerous cutting-edge technologies, such as cloud-enabled real-time *Mobile App* based fire warning systems, Internet of Things (IoT) sensor placement, Unmanned Aerial Vehicle (UAV) technology, integration of GIS and RS-and machine learning-based forest vulnerability susceptibility mapping etc. should be implemented for the quick mitigation of forest fire. To prevent the illegal hunting, deforestation and poaching of animals, the government should enact strict regulations. This includes restricting the number of camping sites and prohibiting the use of picnic areas inside the forest. Moreover, the authorities should keep an eye on the activities of the forest dwellers and their fringe communities during the collection of forest products. They should refrain from allowing the use of match boxes, bidi/cigarettes, and electric transformers. The government should also create awareness about the significance of forest resources by promoting the development of man-made forests, parks, reservoir beatification and implementing joint forest management strategies. These strategies can help to reduce the dependence on forests and improve the living conditions of forest dwellers.

The paper concentrated on a small area, where there is less distribution of the parameters. Hence, for wider applicability of the study results, more studies may be required for the successful identification and mapping of forest fires. The susceptibility models' accuracy might be affected since they were built using geo-environmental information collected for a specific time period. This type of data may change frequently (Solar radiation, rainfall, wind speed, LST etc.), so, susceptibility maps should be regularly updated. The complexity of the model's creation (which is mainly due to its computation time) would have been intriguing. The 44 individual factors that used to make up the framework represented a vast amount of computation space, leading to complex outputs. This could be solved by altering the input configuration. It is sometimes very hard to collect important data and establish crucial elements in the study area due to its uncertain nature and specificity. The accuracy validation of a given model is uncertain when only the ROC curve is used. Therefore, parameters such as kappa coefficient, accuracy, specificity etc. were to evaluate the model outputs.

5. Conclusion

This study addressed the significant impact of forest fires on the STR region, emphasizing the loss of vital resources and biodiversity. Using ten ML models, FFS maps were created, incorporating forty-four ignition factors grouped into six categories. Through rigorous training and testing, the models consistently identified the northern and southern STR areas as being highly susceptible to forest fires. Boruta sensitivity and SHAP evaluations pinpointed twenty-nine influential parameters. Notably, the RF-PSO, nnet, and RF-GWO models demonstrated

exceptional accuracy in delineating fire-prone zones. This study also projected future forest fire zones for 2100, offering invaluable insights for strategic planning. In conclusion, this comprehensive study not only highlights the imminent dangers posed by forest fires but also empowers stakeholders with the knowledge and tools necessary to implement strategic interventions. In doing so, it contributes significantly to the collective endeavour aimed at fortifying the STR against future forest fire challenges.

Funding

The author(s) received no financial support for the research, authorship, and/or publication of this article.

CRediT authorship contribution statement

Swain Sanjay Kumar: Conceptualization, Data curation, Formal analysis, Supervision, Validation, Writing – review & editing. **Swain Kishore Chandra:** Conceptualization, Data curation, Investigation, Methodology, Resources, Validation, Writing – review & editing. **Singha Chiranjit:** Conceptualization, Data curation, Formal analysis, Investigation, Methodology, Software, Visualization, Writing – original draft. **Foroughnia Fatemeh:** Conceptualization, Investigation, Software, Validation, Writing – review & editing. **Moghimi Armin:** Conceptualization, Data curation, Formal analysis, Investigation, Methodology, Supervision, Validation, Visualization, Writing – original draft, Writing – review & editing.

Declaration of Competing Interest

The authors declare that they have no known competing financial interests or personal relationships that could have appeared to influence the work reported in this paper.

Data availability

Data will be made available on request.

Appendix A. Supporting information

Supplementary data associated with this article can be found in the online version at doi:10.1016/j.foreco.2024.121729.

References

Abdollahi, A., Pradhan, B., 2023. Explainable artificial intelligence (XAI) for interpreting the contributing factors feed into the wildfire susceptibility prediction model. Sci. Total Environ. 879, 163004.

Achu, A.L., Thomas, J., Aju, C.D., Gopinath, G., Kumar, S., Reghunath, R., 2021. Machine-learning modelling of fire susceptibility in a forest–agriculture mosaic landscape of southern India. Ecol. Inf. 64, 101348 https://doi.org/10.1016/j.ecoinf.2021.101348.

Akıncı, H.A., Akıncı, H., 2023. Machine learning based forest fire susceptibility assessment of Manavgat district (Antalya), Turkey. Earth Sci. Inf. 16, 397–414. https://doi.org/10.1007/s12145-023-00953-5.

Amani, M., Ghorbanian, A., Ahmadi, S.A., Kakooei, M., Moghimi, A., Mohammm, S., et al., 2020. Google earth engine cloud computing platform for remote sensing big data applications: a comprehensive review, 2020 IEEE J. Sel. Top. Appl. Earth Obs. Remote Sens. 13, 5326–5350. https://doi.org/10.1109/JSTARS.2020.3021052.

Arca, D., Hacısalihoğlu, M., Kutoğlu, Ş.H., 2020. Producing FFS map via multi-criteria decision analysis and frequency ratio methods. Nat. Hazards 104, 73–89. https://doi.org/10.1007/s11069-020-04158-7.

Asadi, S., Roshan, S., Kattan, M.W., 2021. Random forest swarm optimization-based for heart disease diagnosis. J. Biomed. Inf. 115, 103690 https://doi.org/10.1016/j.jbi.2021.103690.

Azmoon, B., Biniyaz, A., Liu, Z., 2022. Use of high-resolution multi-temporal DEM data for landslide detection. Geosciences 12 (10). https://doi.org/10.3390/geosciences12100378.

Babu, K.N., Gour, R., Ayushi, K., Ayyappan, N., Parthasarathy, N., 2023. Environmental drivers and spatial prediction of forest fires in the Western Ghats biodiversity hotspot, India: An ensemble machine learning approach. For. Ecol. Manag. 540, 12105. https://doi.org/10.1016/j.foreco.2023.121057.

Barnard, T.D., Catto, J.L., Harper, A.B., Imron, M.A., van Veen, F.J.F., 2023. Future fire risk under climate change and deforestation scenarios in tropical Borneo. Environ. Res. Lett. 18, 024015.

Bowman, M.J.S.D., Moreira-Munoz, A., Kolden, C.A., Chavez, R.O., Munoz, A.A., Salinas, F., Gonzalez-Reyes, A., Rocco, R., de la Barrera, F., Williamson, G.J., Borchers, N., Cifuentes, L.A., Abatzoglou, J.T., Johnston, F.H., 2018. Human-environmental drivers and impacts of the globally extreme 2017 Chilean fires. Ambio. https://doi.org/10.1007/s13280-018-1084-1.

Breiman, L., 2001. Random forests. Mach. Learn. 45, 5–32 (Jg., S).

Bui, D.T., Ngo, P.T.T., Pham, T.D., Jaafari, A., Minh, N.Q., Hoa, P.V., Samui, P., 2019. A novel hybrid approach based on a swarm intelligence optimized extreme learning machine for flash flood susceptibility mapping. Catena 179, 184–196.

Bustillo Sánchez, M., Tonini, M., Mapelli, A., Fiorucci, P., 2021. Spatial Assessment of Wildfires Susceptibility in Santa Cruz (Bolivia) Using Random Forest. Geosciences 11, 224. https://doi.org/10.3390/geosciences11050224.

Chen, S. , 2021. Interpretation of Multi-label Classification Models Using Shapley Values, 1–12. ⟨https://arxiv.org/abs/2104.10505⟩.

Chen, Y., Ma, L., Yu, D., Zhang, H., Feng, K., Wang, X., Song, J., 2022. Comparison of feature selection methods for mapping soil organic matter in subtropical restored forests. Ecol. Indic. 135, 108545 https://doi.org/10.1016/j.ecolind.2022.108545.

Das, S., Suganthan, P.N., 2011. Differential evolution: a survey of the state-of-the-art. IEEE Trans. Evol. Comput. 15 (1), 4–31.

Dash, M., Behera, B., 2018. Biodiversity conservation, relocation and socio-economic consequences: a case study of Similipal Tiger Reserve, India. Land Use Policy 78, 327–337. https://doi.org/10.1016/j.landusepol.2018.06.030.

Dos Reis, M., Graça, P.M.L. de A., Yanai, A.M., Ramos, C.J.P., Fearnside, P.M., 2021. Forest fires and deforestation in the central Amazon: effects of landscape and climate on spatial and temporal dynamics. J. Environ. Manag. 288, 112310 https://doi.org/10.1016/j.jenvman.2021.112310.

Elyan, E., Gaber, M.M., 2017. A genetic algorithm approach to optimizing random forests applied to class engineered data. Inf. Sci. 384, 220–234. https://doi.org/10.1016/j.ins.2016.08.007.

Eskandari, S., Khoshnevis, M., 2020. Evaluating and mapping the fire risk in the forests and rangelands of sirachal using fuzzy analytic hierarchy process and GIS. For. Res. Dev. 6, 219–245.

Eskandari, S., Pourghasemi, H.R., Miesel, J.R., 2020. The temporal and spatial relationships between climatic parameters and fire occurrence in northeastern Iran. Ecol. Indic. 118, 106720 https://doi.org/10.1016/j.ecolind.2020.106720.

Flannigan, M.D., Stock, B.J., Wotton, B.M., 2000. Climate change and forest fires. Sci. Total Environ. 262, 221–229.

Freund, Y. , Schapire, R.E. , 1996. Experiments with a new boosting algorithm. In Proceedings of the Thirteenth International Conference on Machine Learning, 148–156, Morgan Kauf.

Gallo, C., Eden, J.M., Dieppois, B., Drobyshev, I., Fulé, P.Z., San-Miguel-Ayanz, J., Blackett, M., 2023. Evaluation of CMIP6 model performances in simulating fire weather spatiotemporal variability on global and regional scales. Geosci. Model Dev. 16 (10), 3103–3122. https://doi.org/10.5194/gmd-2022-223.

Gholamnia, K., Nachappa, T.H.G., Ghorbanzadeh, O., Blaschke, T., 2020. Comparisons of diverse machine learning approaches for wildfire susceptibility mapping. Symmetry 12 (4), 604. https://doi.org/10.3390/sym12040604.

Ghorbanzadeh, O., Valizadeh, K.K., Blaschke, T., Aryal, J., Naboureh, A., Einali, J., Bian, J., 2019. Spatial prediction of wildfire susceptibility using field survey GPS data and machine learning approaches. Fire 2 (3), 43. https://doi.org/10.3390/fire2030043.

Gong, J., Jin, T., Cao, E., Wang, S., Yan, L., 2022. Is ecological vulnerability assessment based on the VSD model and AHP-Entropy method useful for loessial forest landscape protection and adaptative management? A case study of Ziwuling Mountain Region, China. Ecol. Indic. 143, 109379 https://doi.org/10.1016/j.ecolind.2022.109379.

Guo, X., Fu, B., Du, J., Shi, P., Chen, Q., Zhang, W., 2021. Applicability of susceptibility model for rock and loess earthquake landslides in the eastern Tibetan plateau. Remote Sens. 13 (13), 2546.

Halofsky, J.E., Peterson, D.L., Harvey, B.J., 2020. Changing wildfire, changing forests: the effects of climate change on fire regimes and vegetation in the Pacific Northwest, USA. Fire Ecol. 16, 4 https://doi.org/10.1186/s42408-019-0062-8.

Hanberry, B.B., 2020. Classifying large wildfires in the United States by Land Cover. Remote Sens. 12, 2966. https://doi.org/10.3390/rs12182966.

Iban, M.C., Sekertekin, A., 2022. Machine learning based wildfire susceptibility mapping using remotely sensed fire data and GIS: A case study of Adana and Mersin provinces, Turkey, 2022,101647 Ecol. Inf. 69. https://doi.org/10.1016/j.ecoinf.2022.101647.

Jaafari, A., Zenner, E.K., Pham, B.T., 2018. Wildfire spatial pattern analysis in the Zagros Mountains, Iran: a comparative study of decision tree based classifiers. Ecol. Inform. 43, 200–211. https://doi.org/10.1016/j.ecoinf.2017.12.006.

Jain, P. , Coogan, S.C.P. , Subramanian, S.G. , Crowley, M. , Taylor, S. , Flannigan, M.D. , 2020. A review of machine learning applications in wildfire science and management. arXiv 2020, arXiv:2003.00646.

Kantarcioglu, O., Schindler, K., Kocaman, S., 2023. Forest fire susceptibility assessment with machine learning methods in north-east Turkiye. Int. Arch. Photogramm. Remote Sens. Spat. Inf. Sci. XLVIII-M-1-2023, 161–167. https://doi.org/10.5194/isprs-archives-XLVIII-M-1-2023-161-2023.

Keenan, R.J., 2015. Climate change impacts and adaptation in forest management: a review. Ann. For. Sci. 72, 145–167. https://doi.org/10.1007/s13595-014-0446-5.

Kerr, G.H., DeGaetano, A.T., Stoof, C.R., Ward, D., 2018. Climate change effects on wildland fire risk in the Northeastern and Great Lakes states predicted by a downscaled multi-model ensemble. Theor. Appl. Climatol. 131, 625–639.

Lamat, R., Kumar, M., Kundu, A., Lal, D., 2021. Forest fire risk mapping using analytical hierarchy process (AHP) and earth observation datasets: a case study in the mountainous terrain of Northeast India, 425 (2021). SN Appl. Sci. 3. https://doi.org/10.1007/s42452-021-04391-0.

Lee, D., Mulrow, J., Haboucha, C.J., Derrible, S., Shiftan, Y., 2019. Attitudes on autonomous vehicle adoption using interpretable gradient boosting machine. Transp. Res Rec. 2673 (11), 865–878.

Li, J., Wang, Y., Nguyen, X., Zhuang, X., Li, J., Querol, X., Li, B., Moreno, N., Hoang, V., Cordoba, P., et al., 2022. First insights into mineralogy, geochemistry, and isotopic signatures of the Upper Triassic high sulfur coals from the Thai Nguyen Coal field, NE Vietnam. Int. J. Coal Geol. 261, 104097.

Li, T., Ni, B., Wu, X., Gao, Q., Li, Q., Sun, D., 2016. On random hyper-class 635 random forest for visual classification. Neurocomputing 172, 281–289 (URL). ⟨http://www.sciencedirect.com/science/article/pii/S0925231215005901⟩.

Li, Y., Li, C., Li, M., Liu, Z., 2019. Influence of variable selection and forest type on forest aboveground biomass estimation using machine learning algorithms. Forests 10, 1073. https://doi.org/10.3390/f10121073.

Mabdeh, A.N., Al-Fugara, A., Khedher, K.M., Mabdeh, M., Al-Shabeeb, A.R., Al-Adamat, R., 2022. FFS assessment and mapping using support vector regression and adaptive neuro-fuzzy inference system-based evolutionary algorithms. Sustainability 14, 9446. https://doi.org/10.3390/su14159446.

Mirjalili, S., Mirjalili, S.M., Lewis, A., 2014. Grey wolf optimizer. Adv. Eng. Softw. 69, 46–61.

Moayedi, H., Khasmakhi, M.A.S.A., 2023. Wildfire susceptibility mapping using two empowered machine learning algorithms. Stoch. Environ. Res. Risk Assess. 37, 49–72. https://doi.org/10.1007/s00477-022-02273-4.

Moayedi, H., Mehrabi, M., Bui, D.T., Pradhan, B., Foong, L.K., 2020. Fuzzy-metaheuristic ensembles for spatial assessment of forest fire susceptibility. J. Environ. Manag., 109867 https://doi.org/10.1016/j.jenvman.2019.109867.

Modugno, S., Balzter, H., Cole, B., Borrelli, P., 2016. Mapping regional patterns of large forest fires in Wildland–Urban Interface areas in Europe. J. Environ. Manag. 172, 112–126. https://doi.org/10.1016/j.jenvman.2016.02.013.

Mohajane, M., Costache, R., Karimi, F., Pham, Q.B., Essahlaoui, A., Nguyen, H., Laneve, G., Oudija, F., 2021. Application of remote sensing and machine learning algorithms for forest fire mapping in a Mediterranean area. Ecol. Indic. 129, 107869.

Mohajane, M., Costache, R., Karimi, F., Pham, Q.B., Essahlaoui, A., Nguyen, H., Laneve, G., Oudija, F., 2021. Application of remote sensing and machine learning algorithms for forest fire mapping in a Mediterranean area. Ecol. Indic. 129, 107869 https://doi.org/10.1016/j.ecolind.2021.107869.

Mutthulakshmi, K., Rui, M., Wee, E., Chong, Y., Wong, K., Cheong, K.H., 2020. Simulating forest fire spread and fire-fighting using cellular automata. Chin. J. Phys. 65, 642–650.

Naderpour, M., Rizeei, H.M., Ramezani, F., 2021. Forest fire risk prediction: a spatial deep neural network-based framework. Remote Sens 13, 2513.

Nuryanto, D.E., Pradana, R.P., Putra, I.D.G.A., Heriyanto, E., Linarka, U.A., Satyaningsih, R., Hidayanto, N., Sopaheluwakan, A., Permana, D.S., 2021. Developing models to establish seasonal forest fire early warning system. IOP Conf. Ser. Earth Environ. Sci. 909, 012005.

Ozalp, Y., Ayse, Halil Akinci, Zeybek, Mustafa, 2023. Comparative analysis of tree-based ensemble learning algorithms for landslide susceptibility mapping: a case study in Rize, Turkey. Water 15 (14), 2661. https://doi.org/10.3390/w15142661.

Papa, J.P., Pagnin, A., Schellini, S.A., Spadotto, A., Guido, R.C., Ponti, M., Falcao, A.X., 2011. Feature selection through gravitational search algorithm. 011 IEEE Int. Conf. Acoust., Speech Signal Process. (ICASSP) 2. https://doi.org/10.1109/icassp.2011.5946916.

Pham, B.T., Jaafari, A., Avand, M., Al-Ansari, N., Dinh Du, T., Yen, H.P.H., Phong, T.V., Nguyen, D.H., Le, H.V., Mafi-Gholami, D., et al., 2020. Performance evaluation of machine learning methods for forest fire modeling and prediction. Symmetry 12, 1022. https://doi.org/10.3390/sym12061022.

Piao, Y., Lee, D., Park, S., Kim, H.G., Jin, Y., 2022. Forest fire susceptibility assessment using google earth engine in Gangwon-do, Republic of Korea. Geomat. Natl. Hazards Risk 13 (1), 432–450. ⟨https://doi. org/10.1080/19475705.2022.2030808⟩.

Pourghasemi, H.R., Gayen, A., Lasaponara, R., Tiefenbacher, J.P., 2020. Application of learning vector quantization and different machine learning techniques to assessing forest fire influence factors and spatial modelling. Environ. Res. 184, 109321.

Pourtaghi, Z.S., Pourghasemi, H.R., Aretano, R., Semeraro, T., 2016. Investigation of general indicators influencing on forest fire and its susceptibility modeling using different data mining techniques. Ecol. Indic. 64, 72–84. https://doi.org/10.1016/j.ecolind.2015.12.030.

Rao, K., Williams, A.P., Flefil, J.F., Konings, A.G., 2020. SAR-enhanced mapping of live fuel moisture content. Remote Sens Environ. 245, 111797 https://doi.org/10.1016/j.rse.2020.111797.

Rashedi, E., Nezamabadi-Pour, H., Saryazdi, S., 2009. GSA: a gravitational search algorithm. Inf. Sci. 179 (13), 2232–2248.

Rihan, M., Bindajam, A.A., Talukdar, S., Shahfahad, Naikoo, M.W., Mallick, J., Rahman, A., 2023. Forest fire susceptibility mapping with sensitivity and uncertainty analysis using machine learning and deep learning algorithms. Adv. Space Res. 72 (2), 426–443. https://doi.org/10.1016/j.asr.2023.03.026.

Saha, S., Bera, B., Shit, P.K., Bhattacharjee, S., Sengupta, N., 2023. Prediction of forest fire susceptibility applying machine and deep learning algorithms for conservation priorities of forest resources. Remote Sens Appl.: Soc. Environ. 29, 100917 https://doi.org/10.1016/j.rsase.2022.100917.

Saranya, K.R., Reddy, C.S., Rao, P.V., Jha, C.S., 2014. Decadal time-scale monitoring of forest fires in Similipal Biosphere Reserve, India using remote sensing and GIS. Environ. Monit. Assess. 186 (5), 3283–3296.

Shabani, S., Reza, H., Blaschke, T., 2020. Forest stand susceptibility mapping during harvesting using logistic regression and boosted regression tree machine learning models. Glob. Ecol. Conserv. 22, e00974 https://doi.org/10.1016/j.gecco.2020.e00974.

Sharma, L.K., Gupta, R., Naureen Fatima, N., 2022. Assessing the predictive efficacy of six machine learning algorithms for the susceptibility of Indian forests to fire. Int. J. Wild. Fire 31 (8), 735–758. https://doi.org/10.1071/WF22016.

Shi, C., Zhang, F., 2023. A forest fire susceptibility modeling approach based on integration machine learning algorithm. Forests 14, 1506. https://doi.org/10.3390/f14071506.

Shmuel, A., Heifetz, E., 2022. Global wildfire susceptibility mapping based on machine learning models. Forests 13, 1050. https://doi.org/10.3390/f13071050.

Simioni, G., Marie, G., Davi, H., Martin-St Paul, N., Huc, R., 2020. Natural forest dynamics have more influence than climate change on the net ecosystem production of a mixed Mediterranean forest. Ecol. Model. 416, 108921 https://doi.org/10.1016/j.ecolmodel.2019.108921.

Singh, K.R., Neethu, K.P., Madhurekaa, K., Harita, A., Mohan, P., 2021. Parallel SVM model for forest fire prediction. Soft Comput. Lett. 3, 100014 https://doi.org/10.1016/j.socl.2021.100014.

Singha, C., Swain, K.C., Meliho, M., Abdo, H.G., Almohamad, H., Al-Mutiry, M., 2022. Spatial analysis of flood hazard zoning map using novel hybrid machine learning technique in Assam, India. Remote Sens. 14, 6229. https://doi.org/10.3390/rs14246229.

Singha, C., Gulzar, S., Swain, K.C., Pradhan, D., 2023. Apple yield prediction mapping using machine learning techniques through the Google Earth Engine cloud in Kashmir Valley, India. J. Appl. Remote Sens. 17 (1), 014505 https://doi.org/10.1117/1.JRS.17.014505.

Sivrikaya, F., Küçük, Ö., 2022. Modeling forest fire risk based on GIS-based analytical hierarchy process and statistical analysis in Mediterranean region. Ecol. Indic. 68, 101537 https://doi.org/10.1016/j.ecoinf.2021.101537.

Sulova, A., Joker Arsanjani, J., 2021. Exploratory analysis of driving force of wildfires in Australia: An application of machine learning within Google Earth Engine. Remote Sens 13 (1), 10. https://doi.org/10.3390/rs13010010.

Sun, Y., Zhang, F., Lin, H., Xu, S., 2022. A forest fire susceptibility modeling approach based on light gradient boosting machine algorithm. Remote Sens 14, 4362. https://doi.org/10.3390/rs14174362.

Tang, X., Machimura, T., Li, J., Liu, W., Hong, H., 2020. A novel optimized repeatedly random undersampling for selecting negative samples: A case study in an SVM-based forest fire susceptibility assessment. J. Environ. Manag. 271, 111014 https://doi.org/10.1016/j.jenvman.2020.111014.

Tavakkoli, P.S., Einali, G., Ghorbanzadeh, O., Nachappa, T.G., Ghamisi, P., Blaschke, T., 2022. A Google Earth Engine Approach for Wildfire Susceptibility Prediction Fusion with Remote Sensing Data of Different Spatial Resolutions. Remote Sens 14, 672. https://doi.org/10.3390/rs14030672.

Tehrany, M.S., Jones, S., Shabani, F., Martínez-Álvarez, F., Tien Bui, D., 2019. A novel ensemble modeling approach for the spatial prediction of tropical forest fire susceptibility using LogitBoost machine learning classifier and multi-source geospatial data. Theor. Appl. Climatol. 137, 637–653.

Thrasher, B., Maurer, E.P., McKellar, C., Duffy, P.B., 2012. Technical Note: Bias correcting climate model simulated daily temperature extremes with quantile mapping. Hydrol. Earth Syst. Sci. 16 (9), 3309–3314. https://doi.org/10.5194/hess-16-3309-2012.

Tien, D., Hoang, N., Samui, P., 2019. Spatial pattern analysis and prediction of forest fire using new machine learning approach of multivariate adaptive regression splines and differential flower pollination optimization: A case study at Lao Cai province (Vietnam). J. Environ. Manag. 237, 476–487.

Times of India. 2021. ⟨https://timesofindia.indiatimes.com/city/dehradun/as-similipal-blaze-hits-8th-daycross-country-forest-fire-alerts-up-125/articleshow/81336308.cms⟩. (Accessed on 21 June 2023).

Tiwari, A., Shoab, M., Dixit, A., 2021. GIS-based FFS modeling in Pauri Garhwal, India: a comparative assessment of frequency ratio, analytic hierarchy process and fuzzy modeling techniques. Nat. Hazards 105, 1189–1230. https://doi.org/10.1007/s11069-020-04351-8.

Trucchia, A., Meschi, G., Fiorucci, P., Gollini, A., Negro, D., 2022. Defining wildfire susceptibility maps in Italy for understanding seasonal wildfire regimes at the national level. Fire 5 (1), 30. ⟨https://doi. org/10.3390/fire5010030⟩.

Zema, D.A., Nunes, J.P., Lucas-Borja, M.E., 2020. Improvement of seasonal runoff and soil loss predictions by the MMF (Morgan-Morgan-Finney) model after wildfire and soil treatment in Mediterranean forest ecosystems. Catena 188, 104415. https://doi.org/10.1016/j.catena.2019.104415.

Zhang, Y., Luo, J., Li, J., Mao, D., Zhang, Y., Huang, Y., Yang, J., 2021. Fast inverse-scattering reconstruction for airborne high-squint radar imagery based on Doppler centroid compensation. IEEE Trans. Geosci. Remote Sens. 60, 1–17.

Zhao, L., Du, M., Du, W., Guo, J., Liao, Z., Kang, X., Liu, Q., 2022. Evaluation of the Carbon Sink Capacity of the Proposed Kunlun Mountain National Park. Int. J. Environ. Res. Public Health 19, 9887.

Zhu, J., Zou, H., Rosset, S., Hastie, T., 2009. Multi-class AdaBoost. Stat. Its Interface 2, 349–360.

Zumbrunnen, T., Menendez, P., Bugmann, H., Conedera, M., Gimmi, U., Bürgi, M., 2012. Human impacts on fire occurrence: a case study of hundred years of forest fires in a dry alpine valley in Switzerland. Reg. Environ. Chang 12, 935–949.